TABLE 2 Genotypic association analysis of *HLA-DRB1* with disease susceptibility

DRB1 genotype	No. of subjects (%)		OR (95% CI)	*P*-value
	Cases	Controls		
SLE	*n* = 656	*n* = 911		
*08:02/*15:01	9 (1.4)	7 (0.8)	2.73 (1.00, 7.41)	0.041
*09:01/*15:01	49 (7.5)	14 (1.5)	7.42 (4.02, 13.71)	3.6×10^{-13}
*08:02/*09:01	21 (3.2)	11 (1.2)	4.05 (1.92, 8.53)	8.2×10^{-5}
*15:01/*15:01	4 (0.6)	5 (0.5)	1.69 (0.33, 7.95)	0.48
*15:01/X[a]	115 (17.5)	96 (10.5)	2.54 (1.86, 3.47)	2.8×10^{-9}
*08:02/*08:02	2 (0.3)	0 (0)	-	0.104
*08:02/X	47 (7.2)	46 (5.0)	2.17 (1.40, 3.35)	4.0×10^{-4}
*09:01/*09:01	28 (4.3)	25 (2.7)	2.37 (1.35, 4.16)	0.0020
*09:01/X	147 (22.4)	211 (23.2)	1.48 (1.14, 1.92)	0.0034
X/X	234 (35.7)	496 (54.4)	Reference	
RA	*n* = 2410	*n* = 911		
SE/*09:01	277 (11.5)	70 (7.7)	3.36 (2.49, 4.54)	3.4×10^{-16}
SE/SE	351 (14.6)	45 (4.9)	6.63 (4.71, 9.34)	1.1×10^{-31}
SE/Y[b]	928 (38.5)	270 (29.6)	2.90 (2.38, 3.54)	1.4×10^{-26}
*09:01/*09:01	90 (3.7)	25 (2.7)	3.03 (1.90, 4.83)	1.4×10^{-6}
*09:01/Y	370 (15.4)	166 (18.2)	1.86 (1.47, 2.35)	1.9×10^{-7}
Y/Y	394 (16.3)	335 (36.8)	Reference	

[a]X: alleles other than *DRB1**08:02, *09:01 and *15:01. [b]Y: alleles other than *DRB1*-SE and *09:01.

TABLE 3 *HLA-DRB1* genotype and the age at disease onset in SLE and RA patients

DRB1 genotype	Total patients			Only female patients		
	No. of subjects	Age at onset, mean (S.D.)	*P*-value[a]	No. of subjects	Age at onset, mean (S.D.)	*P*-value[a]
SLE						
*08:02/*15:01	9	26.7 (10.8)	0.45	8	24.6 (9.5)	0.28
*09:01/*15:01	44	24.3 (11.4)	4.3×10^{-4}	37	24.7 (11.4)	0.0037
*08:02/*09:01	15	33.7 (16.0)	0.63	13	36.3 (15.7)	0.15
*15:01/*15:01	3	27.3 (5.5)	0.87	1	22[b]	1.0
*15:01/X[c]	97	29.9 (13.5)	0.49	88	29.5 (12.8)	0.59
*08:02/*08:02	1	20[b]	1.0	1	20[b]	1.0
*08:02/X	39	31.5 (11.8)	0.57	35	31.4 (12.0)	0.48
*09:01/*09:01	20	30.4 (13.6)	0.99	18	28.2 (9.4)	0.83
*09:01/X	122	29.8 (14.4)	0.36	113	29.0 (13.5)	0.40
X/X	191	30.9 (12.9)	Reference	170	30.0 (11.7)	Reference
RA						
SE/*09:01	264	47.1 (14.2)	2.4×10^{-4}	217	45.8 (14.4)	2.3×10^{-4}
SE/SE	327	47.2 (13.9)	1.0×10^{-4}	256	46.4 (13.6)	0.0012
SE/Y[d]	871	50.2 (14.7)	0.19	709	48.9 (14.6)	0.17
*09:01/*09:01	90	48.5 (13.8)	0.086	76	47.2 (13.5)	0.080
*09:01/Y	335	49.0 (14.5)	0.025	273	48.0 (13.9)	0.056
Y/Y	376	51.4 (14.7)	Reference	316	50.3 (14.9)	Reference

[a]Mann–Whitney *U* test was used. [b]Data of a single patient. [c]X: alleles other than *DRB1**08:02, *09:01 and *15:01. [d]Y: alleles other than *DRB1*-SE and *09:01.

TABLE 4 Association of *HLA-DRB1* genotype and autoantibody status in SLE patients

DRB1 genotype	No. of positive/negative patients (positive rate %)	OR (95% CI)	*P*-value
Anti-dsDNA antibody			
*08:02/*15:01	9/0 (100)	-	1.0
*09:01/*15:01	41/1 (97.6)	2.23 (0.30–99.53)	0.69
*08:02/*09:01	16/1 (94.1)	0.87 (0.11–40.29)	1.0
*15:01/*15:01 or X[a]	93/9 (91.2)	0.56 (0.22–1.44)	0.23
*08:02/*08:02 or X	36/2 (94.7)	0.98 (0.20–9.61)	1.0
*09:01/*09:01 or X	119/22 (84.4)	0.30 (0.14–0.65)	0.0014
X/X	183/10 (94.8)	Reference	
Anti-Sm antibody			
*08:02/*15:01	1/6 (14.3)	0.39 (0.008–3.35)	0.67
*09:01/*15:01	11/24 (31.4)	1.07 (0.48–2.36)	0.87
*08:02/*09:01	6/10 (37.5)	1.40 (0.48–4.07)	0.54
*15:01/*15:01 or X	25/55 (31.3)	1.06 (0.59–1.90)	0.85
*08:02/*08:02 or X	13/20 (39.4)	1.51 (0.69–3.30)	0.30
*09:01/*09:01 or X	58/70 (45.3)	1.93 (1.18–3.15)	0.0084
X/X	46/107 (30.1)	Reference	

[a]X: alleles other than *DRB1**08:02, *09:01 and *15:01.

onset of disease as compared with Y/Y ($P = 1.0 \times 10^{-4}$ and 2.4×10^{-4}, respectively) (Table 3).

Association between *DRB1* and autoantibody profile in SLE

Next we examined the difference in autoantibody status between genotypes in SLE patients. Considering that the number of homozygotic patients for *DRB1**08:02, *09:01 and *15:01 was small, a dominant genetic model was used for this analysis. The *DRB1**09:01-bearing genotypes (*09:01/*09:01 or *09:01/X) showed a significant risk for anti-Sm ($P = 0.0084$, OR 1.93), while it showed a protective effect for anti-dsDNA ($P = 0.0014$, OR 0.30) (Table 4). No significant association with autoantibody status was observed for either *DRB1**15:01-bearing genotypes or the *DRB1**09:01/*15:01 heterozygote, although a lack of statistical power was likely.

The relationship observed between *DRB1**09:01 and the status of anti-dsDNA and anti-Sm in the SLE patients prompted us to test whether *HLA-DRB1* affected the autoantibody profiles in SLE. Previously To *et al.* [37] performed a cluster analysis of the autoantibody profiles in European SLE patients and showed that SLE patients could be divided into three distinct clusters: cluster A (anti-Sm and anti-RNP), cluster B (anti-dsDNA, anti-Ro and anti-La) and cluster C (anti-dsDNA, aCL and LAC). Cluster A showed a significantly higher positive rate of anti-Sm antibody and a lower rate of anti-dsDNA antibody than the two other clusters. Therefore we speculated that Japanese SLE patients could also be sub-clustered by autoantibody profiles, where *DRB1* alleles could be involved. We performed k-mean cluster analysis using autoantibody profiles containing anti-dsDNA, anti-Sm antibodies, aCL and LAC. Similar to the results reported, we found three distinct autoantibody clusters (Table 5). The prevalence of each autoantibody was statistically different among clusters, except for the anti-dsDNA antibody for which the difference was marginal. Then we compared each allele frequency of *DRB1**08:02, *09:01 and *15:01 among the three clusters and found that the frequency of *DRB1**09:01 significantly differed among the clusters ($P = 0.010$). In Cluster 1, characterized by a higher positivity rate of anti-Sm and a lower rate of anti-dsDNA, a higher allele frequency of *DRB1**09:01 and lower frequency of *DRB1**15:01 were observed as compared with the other clusters. The allele frequency of *DRB1**09:01 in Cluster 1 was significantly higher than that of Clusters 2 and 3 ($P = 0.0027$ and 0.035 by χ^2 tests, respectively) (Table 5). The approach of replacing missing data with the mean positive rate is one of the established methods [34], but might lead to false-positive findings. Therefore we also performed k-mean cluster analysis based on casewise deletion and identified similar cluster groups and *DRB1**09:01 frequency distributions among the groups. However, the difference of allele frequencies among the clusters was marginal ($P = 0.09$), suggesting that validation studies using larger sample sizes would be required.

Association of *DRB1* and ACPA status in RA and its interaction with smoking

We evaluated the association of *DRB1*-SE alleles as well as *DRB1**09:01 with ACPA status in our population. When genotype frequencies of *DRB1* were compared between ACPA-positive RA patients ($n = 1884$) and negative patients ($n = 501$), the SE-bearing genotypes (SE/SE or SE/Y) as well as *09:01-bearing genotypes (*09:01/*09:01 or *09:01/Y) conferred significantly increased risk of the appearance of ACPA (Table 6). A significant gene dosage effect of SE was observed for the association with ACPA status (SE/SE vs SE/Y, $P = 6.2 \times 10^{-6}$, OR 2.60), while that of *DRB1**09:01 was not significant (*09:01/

Table 5 Cluster analysis of autoantibody profiles in SLE patients

	Cluster 1 Sm ($n=114$)	Cluster 2 dsDNA only ($n=306$)	Cluster 3 dsDNA/CL/LAC ($n=142$)	*P*-value
Autoantibody positivity (%)				
Anti-dsDNA	87.6	91.4	95.4	0.063
Anti-Sm	100	10	38.4	<0.001
aCL	9.2	12.3	100	<0.001
LAC	12.6	13.8	44.1	<0.001
Allele frequency (%)				
*15:01	10.1	14.9	16.2	0.12
*08:02	6.6	5.4	7.4	0.49
*09:01	27.6	18.2	19.7	0.01

CL: cardiolipin.

Table 6 Association of *HLA-DRB1* genotype and ACPA status in RA patients

		No. of patients (%)			
DRB1 genotype	Smoking status	ACPA positive ($n=1884$)	ACPA negative ($n=501$)	OR (95% CI)	*P*-value
SE/*09:01		238 (12.6)	34 (6.8)	4.93 (3.27, 7.44)	1.2×10^{-15}
SE/SE		320 (17.0)	27 (5.4)	8.35 (5.37, 12.98)	1.8×10^{-25}
SE/Y[a]		756 (40.1)	166 (33.1)	3.21 (2.47, 4.17)	4.0×10^{-19}
*09:01/*09:01		71 (3.8)	18 (3.6)	2.78 (1.60, 4.84)	2.0×10^{-4}
*09:01/Y		269 (14.3)	94 (18.8)	2.02 (1.48, 2.75)	7.6×10^{-6}
Y/Y		230 (12.2)	162 (32.3)	Reference	
		$n=1796$	$n=474$		
SE/*0901					
	Ever	67 (3.7)	6 (1.3)	7.60 (3.17, 18.19)	2.7×10^{-7}
	Never	160 (8.9)	26 (5.5)	4.19 (2.57, 6.81)	1.8×10^{-9}
SE/SE					
	Ever	101 (5.6)	5 (1.1)	13.74 (5.40, 34.94)	1.6×10^{-11}
	Never	209 (11.6)	21 (4.4)	6.77 (4.04, 11.34)	3.7×10^{-15}
SE/Y					
	Ever	252 (14.0)	47 (9.9)	3.65 (2.44, 5.45)	8.4×10^{-11}
	Never	470 (26.2)	111 (23.4)	2.88 (2.08, 4.0)	1.1×10^{-10}
*0901/*0901					
	Ever	22 (1.2)	4 (0.8)	3.73 (1.21, 15.32)	0.011
	Never	44 (2.4)	12 (2.5)	2.49 (1.25, 4.96)	0.0076
*0901/Y					
	Ever	88 (4.9)	32 (6.8)	1.87 (1.16, 3.02)	0.0097
	Never	169 (9.4)	59 (12.4)	1.95 (1.32, 2.88)	7.5×10^{-4}
Y/Y					
	Ever	67 (3.7)	51 (10.8)	0.89 (0.57, 1.39)	0.62
	Never	147 (8.2)	100 (21.1)	Reference	

[a]Y: alleles other than *DRB1*-SE and *09:01.

*09:01 vs *09:01/Y, $P=0.27$, OR 1.38). There was no obvious dominant compound effect in neither SE/*09:01 nor *04:05/*09:01 (data not shown).

Next, we assessed gene–environment interactions between smoking and SE or *DRB1**09:01 alleles in developing ACPA. A larger effect on ACPA development was observed in ever smokers than in never smokers, when patients carried double SE alleles (double SE/ever smoker: OR 13.74; double SE/never smoker: OR 6.77) (Table 6). In order to investigate the interactions between smoking and SE or *DRB1**09:01, we examined the interaction terms in a logistic regression model. The logistic coefficient for the interaction term between SE and smoking was significant ($P=0.047$). However, that between *DRB1**09:01 and smoking was not significant ($P=0.34$), although lack of statistical power should be considered.

We also evaluated the interaction between smoking and *DRB1* alleles by calculating the three measures (RERI, AP and S). We found interactions only in SE alleles [double SE: RERI 7.34 (95% CI −6.55, 21.24), AP 0.51 (95% CI 0.01, 1.0), S 2.23 (95% CI 0.72, 6.94); single SE: RERI 1.32 (95% CI −0.35, 2.99), AP 0.31 (95% CI 0.01, 0.61), S 1.68 (95% CI 0.92, 3.06)], but not in *DRB1**09:01 (data not shown).

Discussion

In the present analysis of *HLA-DRB1* locus in Japanese SLE and RA patients using one of the largest cohorts ever examined in Asian populations, we demonstrated that *DRB1* alleles were associated with susceptibility as well as disease subphenotype, where the *DRB1**09:01 allele, prominent in Asian populations, has a significant impact in both diseases.

In SLE, *HLA-DRB1**15:01, *09:01, *08:02 and *04:01 were significantly associated with disease susceptibility in our population, where the association of *08:02 and *04:01 has not been previously described in Asian populations. In contrast to *15:01, we did not observe a significant association in *DRB1**15:02. As the *15:02 allele is rarely observed in European populations, and the majority of previous studies in Asian populations examined these alleles together as DR2 (or DR15) serotypes, the differential role of these two alleles had not been clearly defined. As for the amino acid sequence, these alleles only differ at position 86 (a valine for *DRB1**15:01 and a glycine for *DRB1**15:02). This amino acid constitutes the P1 pocket of the DRβ molecule and is considered to be critical for antigen presentation [38]. The influence of other HLA genes on the haplotype of *DRB1*, such as *DQB1*, should also be considered. In this context, the positive association of *DRB1**15:02 observed in Taiwanese and Thais [39, 40], unlike in our population, could be explained by the primary association of *DQB1**05:01, considering that the *DRB1**15:02 is in strong linkage disequilibrium with *DQB1**06:01, not with *DQB1**05:01, in a Japanese population.

In the genotypic comparison, we found that the compound heterozygote *DRB1**09:01/*15:01 showed a remarkable contribution to increased risk of SLE as well as earlier disease onset. A compound heterozygote of *DRB1* haplotypes may have an increased probability of presenting self-antigens, leading to increased predisposition and earlier onset of disease. Alternatively, the *trans*-complementing heterodimers formed by *DQA* and *DQB* genes on the haplotype of *DRB1**09:01 and *15:01 could also explain the increased effect of heterozygote, as was suggested in a study of Type 1 diabetes (T1D) [41]. In contrast to SLE, no obvious compound heterozygote effect of *DRB1*-SE/*09:01 (or *04:05/*09:01) was observed in RA, possibly because the stronger effect of SE alleles may dominate that of *DRB1**09:01 in RA.

We demonstrated a positive association of *DRB1**09:01 with anti-Sm antibody formation, but a negative association with anti-dsDNA antibody in SLE patients, implying that differential mechanisms involving different DR molecules underlie the appearance of these autoantibodies. A recent study in European patients reported that an SNP in the HLA class II region was associated with anti-dsDNA antibody-negative patients, which may support our findings [42]. To *et al.* [37] found that SLE patients could be grouped into several autoantibody patterns, and one of the groups was characterized by a higher positivity rate of anti-RNP and anti-Sm and a lower rate of anti-dsDNA antibodies. This grouping by autoantibody patterns was also applicable to the population we examined. In addition, as differential distribution of *DRB1* alleles was also observed among the groups in our population, combinations of the class II haplotypes should affect autoantibody production in SLE and may influence clinical subphenotypes of SLE patients.

The association of SE alleles in ACPA-positive RA has been well established in both European and Asian populations [14–16, 18, 19]. This suggests an essential role of the SE alleles in presenting citrullinated self-antigens. In addition, a gene–environment interaction between SE alleles and smoking has been demonstrated for the onset of RA [18, 19]. These suggest a pathological series of smoking, citrullination of self-proteins and antigen presentation by SE alleles [43]. However, whether this is also the case for *DRB1**09:01 is not clear. Two previous studies in Japanese populations suggested that *DRB1**09:01 but not SE alleles is associated with ACPA-negative RA [21, 22]. The study by Furuya *et al.* [21] indicated a significant association of *DRB1**09:01 with ACPA-negative RA ($P = 0.016$, OR 2.2). Another study by Terao *et al.* [22], in which the ACPA-negative patients (502 subjects) used in the present study were also included, showed a marginal association with ACPA-negative RA ($P = 0.062$, OR 1.16). However, the effect of *DRB1**09:01, independent of SE alleles, on ACPA-positive RA was not evaluated in these studies. Another study in a Korean population showed that *DRB1**09:01 made a significant contribution to the appearance of ACPA independently of SE ($P = 1.10 \times 10^{-3}$, OR 2.49) [18], which corresponds to our observation (Table 6). Taken together, this evidence suggests that *DRB1**09:01 confers risk for both ACPA-positive and ACPA-negative RA. Moreover, as no significant gene–environmental interaction was observed between smoking and *DRB1**09:01 for the appearance of ACPA, *DRB1**09:01 may not function in the same pathological series of SE alleles, as mentioned.

The amino acid sequence of *DRB1**09:01 at 70–74 (RRRAE) is different from that of the SE alleles. As both *DRB1**14:05 and *14:54, the only alleles that share the RRRAE epitope in the Japanese population, displayed a negative trend for the risk of RA, it may be unlikely that this epitope alone can explain the susceptibility of *DRB1**09:01 to RA. A recent study examining all possible epitopes in the DR molecule showed that two new epitopes ($VH^{11,13}$ and $LA^{67,74}$) in addition to the classical SE exhibited a predisposition to RA in European populations [44]. Haplotypes involving *DRB1**09:01 have been reported to be associated with autoimmune diseases other than RA and SLE, including T1D, Graves' disease,

mixed CTD and microscopic polyangiitis in Asian populations [45–48], suggesting that these autoimmune diseases share the same pathological pathway. Although the DR9 molecule itself may play an important role in disease pathogenesis, it is also known that *DRB1**09:01 is in linkage with *DRB4*, a paralogue of *DRB1* that also encodes DRβ chains. *DRB4* is only present in haplotypes of *DRB1**04, *07 and *09. Its presence has been found to be associated with the progression of RA [49] and the presence of ACPA [50]. Therefore the association of *DRB1**09:01 could be secondary to the effect of *DRB4* in RA. In addition, the exclusive presence of *DRB4* in *DRB1**04 among SE alleles might explain the difference in the effect size between *DRB1**04 alleles and other SE alleles (i.e. *01:01).

In conclusion, we identified *HLA-DRB1* alleles associated with SLE and RA in a Japanese population and demonstrated a shared susceptibility of *DRB1**09:01 between the diseases as well as its effect on autoantibody production. Further studies, such as structural analysis of the *DRB1**09:01 product itself and analysis of other candidate causal variants of the *DRB1**09:01 haplotype, are needed to clarify the exact role of the *DRB1**09:01 haplotype in disease pathogenesis.

Rheumatology key messages

- A large-scale association study identified *HLA-DRB1* alleles associated with SLE and RA in the Japanese population.
- *HLA-DRB1**09:01 allele is associated with susceptibility to both SLE and RA in the Japanese population.
- *HLA-DRB1**09:01 allele affects autoantibody profiles of SLE and RA in Japanese patients.

Acknowledgements

We are grateful to Dr A. Miyatake, the members of the Rotary Club of Osaka-Midosuji District 2660 Rotary International in Japan, the members of the autoimmune disease study group of Research in Intractable Diseases, Ministry of Health, Labor and Welfare, Japan, and the staffs of the BioBank Japan Project for supporting both the study and clinical sample collection. We also thank K. Kobayashi, M. Kitazato and other members of the Laboratory for Autoimmune Diseases, Center for Genomic Medicine, Institute of Physical and Chemical Research, for their helpful advice and excellent technical assistance.

Funding: This work was supported by a grant from the Center for Genomic Medicine, Institute of Physical and Chemical Research, and a grant from the Japanese Ministry of Health, Labor and Welfare.

Disclosure statement: The authors have declared no conflicts of interest.

References

1 Graham RR, Ortmann WA, Langefeld CD *et al.* Visualizing human leukocyte antigen class II risk haplotypes in human systemic lupus erythematosus. Am J Hum Genet 2002;71:543–53.

2 Barcellos LF, May SL, Ramsay PP *et al.* High-density SNP screening of the major histocompatibility complex in systemic lupus erythematosus demonstrates strong evidence for independent susceptibility regions. PLoS Genet 2009;5:e1000696.

3 Jawaheer D, Li W, Graham RR *et al.* Dissecting the genetic complexity of the association between human leukocyte antigens and rheumatoid arthritis. Am J Hum Genet 2002;71:585–94.

4 Rioux JD, Goyette P, Vyse TJ *et al.* Mapping of multiple susceptibility variants within the MHC region for 7 immune-mediated diseases. Proc Natl Acad Sci USA 2009;106:18680–5.

5 Fernando MM, Stevens CR, Walsh EC *et al.* Defining the role of the MHC in autoimmunity: a review and pooled analysis. PLoS Genet 2008;4:e1000024.

6 Kim I, Kim YJ, Kim K *et al.* Genetic studies of systemic lupus erythematosus in Asia: where are we now? Genes Immun 2009;10:421–32.

7 Li CF, He XH, Teng Q, Jiang ZF. [Association of HLA-A, B, and DR haplotypes with genotype in Chinese children with systemic lupus erythematosus]. Zhonghua Er Ke Za Zhi 2003;41:422–5.

8 Hong GH, Kim HY, Takeuchi F *et al.* Association of complement C4 and HLA-DR alleles with systemic lupus erythematosus in Koreans. J Rheumatol 1994;21:442–7.

9 Zhang J, Ai R, Chow F. The polymorphisms of HLA-DR and TNF B loci in northern Chinese Han nationality and susceptibility to systemic lupus erythematosus. Chin Med Sci J 1997;12:107–10.

10 Lee HS, Chung YH, Kim TG *et al.* Independent association of HLA-DR and FCgamma receptor polymorphisms in Korean patients with systemic lupus erythematosus. Rheumatology 2003;42:1501–7.

11 Hashimoto H, Nishimura Y, Dong RP *et al.* HLA antigens in Japanese patients with systemic lupus erythematosus. Scand J Rheumatol 1994;23:191–6.

12 Gregersen PK, Silver J, Winchester RJ. The shared epitope hypothesis. An approach to understanding the molecular genetics of susceptibility to rheumatoid arthritis. Arthritis Rheum 1987;30:1205–13.

13 Nepom GT, Byers P, Seyfried C *et al.* HLA genes associated with rheumatoid arthritis. Identification of susceptibility alleles using specific oligonucleotide probes. Arthritis Rheum 1989;32:15–21.

14 Huizinga TW, Amos CI, van der Helm-van Mil AH *et al.* Refining the complex rheumatoid arthritis phenotype based on specificity of the HLA-DRB1 shared epitope for antibodies to citrullinated proteins. Arthritis Rheum 2005;52:3433–8.

15 van der Helm-van Mil AH, Verpoort KN, Breedveld FC *et al.* The HLA-DRB1 shared epitope alleles are primarily a risk factor for anti-cyclic citrullinated peptide antibodies and are not an independent risk factor for development of rheumatoid arthritis. Arthritis Rheum 2006;54:1117–21.

16 van Gaalen FA, van Aken J, Huizinga TW *et al.* Association between HLA class II genes and autoantibodies to cyclic citrullinated peptides (CCPs) influences the severity of rheumatoid arthritis. Arthritis Rheum 2004;50:2113–21.

17 Linn-Rasker SP, van der Helm-van Mil AH, van Gaalen FA *et al.* Smoking is a risk factor for anti-CCP antibodies only in rheumatoid arthritis patients who carry HLA-DRB1 shared epitope alleles. Ann Rheum Dis 2006; 65:366–71.

18 Bang SY, Lee KH, Cho SK *et al.* Smoking increases rheumatoid arthritis susceptibility in individuals carrying the HLA-DRB1 shared epitope, regardless of rheumatoid factor or anti-cyclic citrullinated peptide antibody status. Arthritis Rheum 2010;62:369–77.

19 Kallberg H, Padyukov L, Plenge RM *et al.* Gene-gene and gene-environment interactions involving HLA-DRB1, PTPN22, and smoking in two subsets of rheumatoid arthritis. Am J Hum Genet 2007;80:867–75.

20 Kochi Y, Yamada R, Kobayashi K *et al.* Analysis of single-nucleotide polymorphisms in Japanese rheumatoid arthritis patients shows additional susceptibility markers besides the classic shared epitope susceptibility sequences. Arthritis Rheum 2004;50:63–71.

21 Furuya T, Hakoda M, Ichikawa N *et al.* Differential association of HLA-DRB1 alleles in Japanese patients with early rheumatoid arthritis in relationship to autoantibodies to cyclic citrullinated peptide. Clin Exp Rheumatol 2007; 25:219–24.

22 Terao C, Ohmura K, Kochi Y *et al.* A large-scale association study identified multiple HLA-DRB1 alleles associated with ACPA-negative rheumatoid arthritis in Japanese subjects. Ann Rheum Dis 2011;70:2134–9.

23 Okada Y, Suzuki A, Yamada R *et al.* HLA-DRB1*0901 lowers anti-cyclic citrullinated peptide antibody levels in Japanese patients with rheumatoid arthritis. Ann Rheum Dis 2010;69:1569–70.

24 Wordsworth P, Pile KD, Buckely JD *et al.* HLA heterozygosity contributes to susceptibility to rheumatoid arthritis. Am J Hum Genet 1992;51:585–91.

25 MacGregor A, Ollier W, Thomson W *et al.* HLA-DRB1*0401/0404 genotype and rheumatoid arthritis: increased association in men, young age at onset, and disease severity. J Rheumatol 1995;22:1032–6.

26 Lee HS, Lee KW, Song GG *et al.* Increased susceptibility to rheumatoid arthritis in Koreans heterozygous for HLA-DRB1*0405 and *0901. Arthritis Rheum 2004;50: 3468–75.

27 Nakamura Y. The BioBank Japan Project. Clin Adv Hematol Oncol 2007;5:696–7.

28 Hochberg MC. Updating the American College of Rheumatology revised criteria for the classification of systemic lupus erythematosus. Arthritis Rheum 1997;40:1725.

29 Arnett FC, Edworthy SM, Bloch DA *et al.* The American Rheumatism Association 1987 revised criteria for the classification of rheumatoid arthritis. Arthritis Rheum 1988; 31:315–24.

30 Okada Y, Yamazaki K, Umeno J *et al.* HLA-Cw*1202-B*5201-DRB1*1502 haplotype increases risk for ulcerative colitis but reduces risk for Crohn's disease. Gastroenterology 2011;141:864–71.

31 Brandt JT, Barna LK, Triplett DA. Laboratory identification of lupus anticoagulants: results of the Second International Workshop for Identification of Lupus Anticoagulants. On behalf of the Subcommittee on Lupus Anticoagulants/Antiphospholipid Antibodies of the ISTH. Thromb Haemost 1995;74:1597–603.

32 Payami H, Joe S, Farid NR *et al.* Relative predispositional effects (RPEs) of marker alleles with disease: HLA-DR alleles and Graves disease. Am J Hum Genet 1989;45: 541–6.

33 Rothman KJ. Epidemiology: an introduction. New York: Oxford University Press, 2002.

34 Katz HM. Multivariable analysis. New York: Cambridge University Press, 1999.

35 Cordell HJ. Detecting gene-gene interactions that underlie human diseases. Nat Rev Genet 2009;10:392–404.

36 Andersson T, Alfredsson L, Kallberg H *et al.* Calculating measures of biological interaction. Eur J Epidemiol 2005; 20:575–9.

37 To CH, Petri M. Is antibody clustering predictive of clinical subsets and damage in systemic lupus erythematosus? Arthritis Rheum 2005;52:4003–10.

38 Jones EY, Fugger L, Strominger JL *et al.* MHC class II proteins and disease: a structural perspective. Nat Rev Immunol 2006;6:271–82.

39 Lu LY, Ding WZ, Fici D *et al.* Molecular analysis of major histocompatibility complex allelic associations with systemic lupus erythematosus in Taiwan. Arthritis Rheum 1997;40:1138–45.

40 Sirikong M, Tsuchiya N, Chandanayingyong D *et al.* Association of HLA-DRB1*1502-DQB1*0501 haplotype with susceptibility to systemic lupus erythematosus in Thais. Tissue Antigens 2002;59:113–7.

41 Erlich H, Valdes AM, Noble J *et al.* HLA DR-DQ haplotypes and genotypes and type 1 diabetes risk: analysis of the type 1 diabetes genetics consortium families. Diabetes 2008;57:1084–92.

42 Chung SA, Taylor KE, Graham RR *et al.* Differential genetic associations for systemic lupus erythematosus based on anti-dsDNA autoantibody production. PLoS Genet 2011;7: e1001323.

43 Klareskog L, Ronnelid J, Lundberg K *et al.* Immunity to citrullinated proteins in rheumatoid arthritis. Annu Rev Immunol 2008;26:651–75.

44 Freed BM, Schuyler RP, Aubrey MT. Association of the HLA-DRB1 epitope LA(67, 74) with rheumatoid arthritis and citrullinated vimentin binding. Arthritis Rheum 2011; 63:3733–9.

45 Murao S, Makino H, Kaino Y *et al.* Differences in the contribution of HLA-DR and -DQ haplotypes to susceptibility to adult- and childhood-onset type 1 diabetes in Japanese patients. Diabetes 2004;53: 2684–90.

46 Tsuchiya N, Kobayashi S, Hashimoto H *et al.* Association of HLA-DRB1*0901-DQB1*0303 haplotype with microscopic polyangiitis in Japanese. Genes Immun 2006;7: 81–4.

47 Huang SM, Wu TJ, Lee TD *et al.* The association of HLA-A, -B, and -DRB1 genotypes with Graves' disease in Taiwanese people. Tissue Antigens 2003;61:154–8.

48 Dong RP, Kimura A, Hashimoto H *et al.* Difference in HLA-linked genetic background between mixed connective tissue disease and systemic lupus erythematosus. Tissue Antigens 1993;41:20–5.

49 Heldt C, Listing J, Sozeri O *et al.* Differential expression of HLA class II genes associated with disease susceptibility and progression in rheumatoid arthritis. Arthritis Rheum 2003;48:2779–87.

50 Engelmann R, Eggert M, Neeck G *et al.* The impact of HLA-DRB alleles on the subclass titres of antibodies against citrullinated peptides. Rheumatology 2010;49:1862–6.

Clinical vignette

Rheumatology 2013;52:1182
doi:10.1093/rheumatology/ket014
Advance Access publication 16 February 2013

Critical reversible bilateral internal carotid artery stenosis associated with SLE

A 44-year-old teacher presented with intense headache. She had mouth ulcers and dry mouth. Investigations revealed positive ANA of 1:160, DNA antibodies of 343 units (positive > 60) and aCL IgG of 26.4 units (<17). Magnetic resonance angiography (MRA) revealed a long irregular stenosis of the left internal carotid artery and a 20% stenosis of the right internal carotid artery (Fig. 1A). Five days later an MRA with different sequences revealed an irregular 80% stenosis of the left internal carotid artery and an irregular stenosis of the right internal carotid artery, a new finding, indicating rapid progression of the disease (Fig. 1B).

The oral ulcers, positive ANA, DNA and aCL IgG antibodies were consistent with SLE [1]. We started prednisolone 60 mg/day and aspirin 75 mg/day and the headache resolved. HCQ and MTX were added. Prednisolone was gradually tapered to 5 mg/day and the MTX was gradually increased to 20 mg weekly. The most recent MRA showed mild irregularity of the left internal carotid artery and a normal right internal carotid artery.

Our patient had headache and critical rapidly progressive reversible bilateral internal carotid artery stenosis associated with SLE. With prompt immunosuppression her symptoms resolved and the radiographic appearance of the carotid arteries improved.

Disclosure statement: The authors have declared no conflicts of interest.

Christakis Christodoulou[1], Charalambos Economides[2] and David D'Cruz[3]

[1]Syneseion Medical Centre, Larnaca, Cyprus, [2]Ayios Therissos Medical Diagnostic Centre, Nicosia, Cyprus and [3]Louise Coote Lupus Unit, Gassiot House, St Thomas' Hospital, London, UK.

Correspondence to: Christakis Christodoulou, Syneseion Medical Centre, Rheumatology, Rafael Santi 15, Larnaca 6052, Cyprus. E-mail: chrisc@doctors.org.uk

Reference

1 Petri M, Orbai A, Alarcon GS *et al.* Derivation and validation of the Systemic Lupus International Collaborating Clinics classification criteria for systemic lupus erythematosus. Arthritis Rheum 2012;64:2677–86.

FIG. 1 MRA scans of the carotids demonstrating critical rapidly progressive bilateral internal carotid artery stenosis.

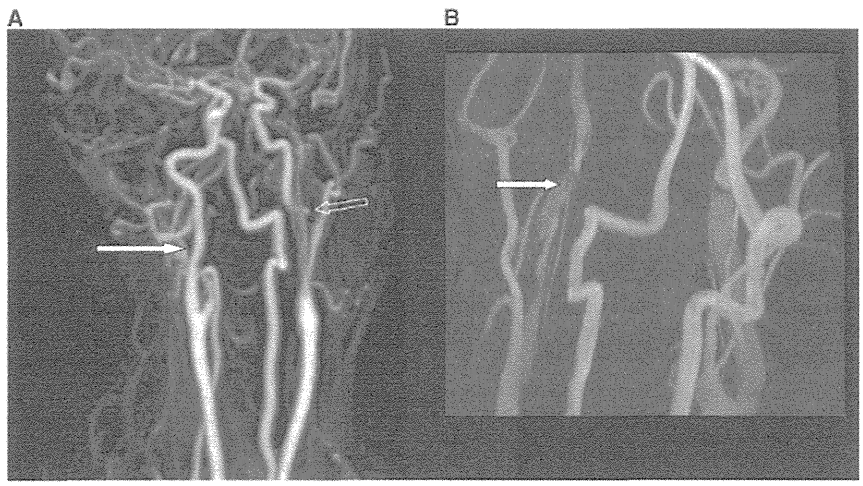

(**A**) MRI/MRA brain and carotids (19 September 2010) showing irregular stenosis of the left internal carotid artery (ICA, open arrow) with an almost normal right internal carotid artery (white arrow). (**B**) Non-contrast MRA 3DI of the carotids with different sequences (24 September 2010) demonstrating irregular stenosis of the right ICA (white arrow), which is a new finding in comparison with the scan in (A).

Cd72^c Is a Modifier Gene that Regulates *Fas*^{lpr}-Induced Autoimmune Disease

Miduo Xu,*,† Rong Hou,*,† Aya Sato-Hayashizaki,*,† Rongyong Man,*,† Chenghua Zhu,*,† Chisato Wakabayashi,*,† Sachiko Hirose,‡ Takahiro Adachi,*,† and Takeshi Tsubata*,†

Although modifier genes are extensively studied in various diseases, little is known about modifier genes that regulate autoimmune diseases. Autoimmune disease caused by the *Fas*^{lpr} mutation depends on the genetic background of mouse strains, suggesting a crucial role of modifier genes. MRL/MpJ-*Fas*^{lpr} (MRL/lpr) and AKR/lpr mice develop severe and mild lupus-like autoimmune disease, respectively, whereas this mutation does not cause disease on C57BL/6 (B6) or C3H background. Both MRL and AKR carry the same haplotype of the *Cd72* gene encoding an inhibitory BCR coreceptor (CD72^c), and CD72^c contains several amino acid substitutions and a deletion in the extracellular region compared with CD72^a and CD72^b. To address the role of *Cd72*^{c} locus in the regulation of *Fas*^{lpr}-induced autoimmune disease, we generated B6.CD72^c/lpr and MRL.CD72^b/lpr congenic mice. Introduction of the chromosomal interval containing *Cd72*^{c} did not cause disease in B6 mice by itself, but caused development of lupus-like disease in the presence of *Fas*^{lpr} on B6 background, clearly demonstrating that this interval contains the modifier gene that regulates *Fas*^{lpr}-induced autoimmune disease. Conversely, MRL.CD72^b/lpr congenic mice showed milder disease compared with MRL/lpr mice. We further demonstrated that *Cd72*^{c} is a hypofunctional allele in BCR signal inhibition and that CD72 deficiency induces severe autoimmune disease in the presence of *Fas*^{lpr}. These results strongly suggest that the *Cd72*^{c} is a crucial modifier gene that regulates *Fas*^{lpr}-induced autoimmune disease due to its reduced activity of B cell signal regulation. ***The Journal of Immunology*, 2013, 190: 5436–5445.**

Modifier genes have been extensively studied in various diseases such as cancer, arrythmia, and cystic fibrosis, because penetrance and disease manifestations of the disease caused by disease-causing genes are extensively modified by modifier genes (1–3). In cystic fibrosis, contribution of modifier genes to the disease variability is almost equivalent to that of environmental factors. Mutation of the *Fas* gene causes autoimmune disease in both mice and human (4–7). Penetrance, severity, and manifestations of the disease induced by *Fas*^{lpr} mutation, a loss-of-function mutation of *Fas*, depend on the genetic background of mouse strains. MRL/MpJ-*Fas*^{lpr} (MRL/lpr) and AKR/lpr mice develop severe and mild lupus-like autoimmune disease, whereas *Fas*^{lpr} does not induce autoimmune disease in C57BL/6 and C3H mice (8, 9). Moreover, Fas-deficient BALB/c mice were recently shown to develop allergic inflammation (10). Thus, the disease caused by *Fas*^{lpr} or Fas deficiency is strongly regulated by modifier genes.

CD72 is a 45-kDa type II membrane protein expressed in B cells. CD72 contains a C-type lectin-like domain in the extracellular region and an immunoreceptor tyrosine-based inhibition motif (ITIM) in the cytoplasmic region (11–13). CD72 negatively regulates BCR signaling by recruiting SH2-containing tyrosine phosphatase-1 at the ITIM (12–16). In mice, four allelic forms of CD72 (i.e., CD72^a, CD72^b, CD72^c, and CD72^d) were serologically defined (17). CD72^a, CD72^b, and CD72^d are highly homologous (18, 19). In contrast, the extracellular region of CD72^c has a marked difference from the other alleles including a 7-aa deletion in the C-type lectin-like domain, although the amino acid sequence of the transmembrane and cytoplasmic regions of CD72^c is identical to that of the other alleles (18, 19). Interestingly, MRL and AKR, both of which develop autoimmune disease in the presence of *Fas*^{lpr}, carry CD72^c, whereas most of the other strains of mice, including BALB/c and C57BL/6 (B6), carry either CD72^a or CD72^b (18, 19). Moreover, studies using microsatellite markers revealed association of the loci containing *Cd72* to development of glomerulonephritis in MRL/lpr mice (20–22). Thus, *Cd72*^{c} is a candidate for a modifier gene that regulates *Fas*^{lpr}-induced autoimmune disease.

In this study, we addressed the role of the *Cd72*^{c} locus in the development of autoimmune disease by generating B6.CD72^c and MRL.CD72^b/lpr congenic mice. B cells from B6.CD72^c congenic mice showed augmented BCR signaling compared with B6 B cells, and B6.CD72^c/lpr developed severe autoimmune disease, whereas B6.CD72^c mice showed no disease. Conversely, MRL.CD72^b/lpr mice showed less severe autoimmune disease compared with MRL/lpr mice. These results suggest that *Cd72*^{c} is a functionally defective allele, and the *Cd72*^{c} locus does not cause any disease by itself but plays a role in development of severe autoimmune disease in MRL/lpr mice probably by augmenting BCR signaling. We further demonstrate that CD72 deficiency causes severe autoimmune disease in the presence of *Fas*^{lpr} by generating CD72-deficient mice. Thus, *Cd72*^{c} is a modifier gene that plays a crucial role in development of *Fas*^{lpr}-induced autoimmune disease probably through its defective regulatory function on BCR signaling.

*Laboratory of Immunology, Graduate School of Biomedical Sciences, Tokyo Medical and Dental University, Tokyo 113-8510, Japan; †Department of Immunology, Medical Research Institute, Tokyo Medical and Dental University, Tokyo 113-8510, Japan; and ‡Department of Pathology, Juntendo University School of Medicine, Tokyo 113-8421, Japan

Received for publication January 2, 2013. Accepted for publication March 27, 2013.

This work was supported in part by grants from the Ministry of Education, Culture, Sports, Science and Technology of Japan and the Japan Society for the Promotion of Science.

Address correspondence and reprint requests to Prof. Takeshi Tsubata, Department of Immunology, Medical Research Institute, Tokyo Medical and Dental University, 1-5-45 Yushima, Bunkyo-ku, Tokyo 113-8510, Japan. E-mail address: tsubata.imm@mri.tmd.ac.jp

The online version of this article contains supplemental material.

Abbreviations used in this article: ALPS, autoimmune lymphoproliferative syndrome; B6, C57BL/6; BAC, bacterial artificial chromosome; BM, bone marrow; ES, embryonic stem; ITIM, immunoreceptor tyrosine-based inhibition motif; LN, lymph node; MRL/lpr, MRL/MpJ-*Fas*^{lpr}; NP, 4-hydroxy-3-nitrophenyl acetyl; PASH, periodic acid–Schiff and hematoxylin; PEC, peritoneal exudate cells.

www.jimmunol.org/cgi/doi/10.4049/jimmunol.1203576

Materials and Methods

Cell lines

The mouse B cell line BAL17 and its transfectants were cultured in RPMI 1640 medium supplemented with 10% FCS, 50 μM 2-ME, 1 mM L-glutamine, and 100 U penicillin/streptomycin. The retrovirus packaging cell line PLAT-E (a gift of Dr. T. Kitamura, University of Tokyo, Tokyo, Japan) (23) was maintained in DMEM supplemented with 10% FCS, 2 mM L-glutamine, and 100 U penicillin/streptomycin. Embryonic stem (ES) cell line R-CMTI-2A derived from B6 mice was purchased from Dainippon Sumitomo Pharma (Osaka, Japan) and was cultured in DMEM medium supplemented with 15% FBS, L-glutamine, nonessential amino acids, and LIF (Chemicon International).

Vector and retrovirus

The $CD72^a$ and $CD72^c$ cDNA was obtained from total RNA prepared from a DBA/2 and MRL/lpr mouse spleen, respectively, by RT-PCR using a set of primers (5′-CCGAATTCATGGCTGACGCTATCACG-3′ and 5′-AAGCGGCCGCTATATCCGGTTCAGTTCAG-3′). These fragments were inserted into the retroviral vector pMX (a gift of Dr. T. Kitamura) (24). For retrovirus production, the packaging cells were transfected with retroviral vectors using a calcium phosphate method. Cells were cultured for 48 h, and the culture supernatant was collected. BAL17 cells were incubated with the supernatant containing retrovirus in the presence of 5 μg/ml polybrene for 4 h.

Mice

B6 and MRL/lpr mice were purchased from Sankyo Laboratory Service (Tokyo, Japan). B6/lpr mice were purchased from Japan SLC (Hamamatsu, Japan). QM mice were as described previously (25) (a kind gift from Dr. M. Wabl, University of California, San Francisco, San Francisco, CA). To generate CD72-dificient mice, genomic DNA fragments containing *Cd72* were isolated by PCR from the bacterial artificial chromosome (BAC) clone derived from a B6 mouse. The targeting vector was constructed by inserting the neomycin resistance gene flanked by the *loxP* sequences upstream of the first exon of *Cd72* (Supplemental Fig. 2A). The linearized targeting vector was transfected by electroporation into the R-CMTI-2A ES cells. The $Cd72^{+/-}$ ES cell clones 4 and 150 (Supplemental Fig. 2B) were used for blastocyst injection to generate chimeric mice. Lack of CD72 expression in $Cd72^{-/-}$ mice was confirmed by flow cytometry and Western blotting (Supplemental Fig. 2C, 2D). All mice used in this study were bred and maintained in a specific pathogen-free animal facility of Tokyo Medical and Dental University and handled according to our institutional guidelines.

Genotyping

Genomic DNA was extracted from mouse tail and genotyping was done by PCR. Microsatellite primers *D4Mit268*, *D4Mit193*, *D4Mit196*, *D4Mit91*, *D4Mit241*, *D4Mit17*, *D4Mit9*, *D4Mit308*, and *D4Mit203*, located at 8.73, 13.99, 20.16, 23.04, 30.48, 33.96, 43.34, 57.66, and 63.26 cM distal from the centromere on chromosome 4, respectively, were synthesized according to Mouse Genome Informatics (The Jackson Laboratory). The $Cd72^b$ and $Cd72^c$ allele were specifically amplified using the following primers sets: $Cd72^b$ forward, 5′-ACATATTACCAGAAGTGGGA-3′ and reverse, 5′-GGTTAAGGATGTAGGTCACAAGGTCTT-3′; and $Cd72^c$ forward, 5′-ATATATAACAAGAAGTGGGC-3′ and reverse, 5′-GGTTAAGGATGTAGGTCACAAGGTCTT-3′. Fas^{WT} and Fas^{lpr} were specifically amplified using the following primers: forward primer, 5′-TTTACTCATTGACTTATCAAGT-3′; reverse primer specific for Fas^{WT}, 5′-AGCCTCCAGGGCCTTCACCTTCTCA-3′; and a reverse primer specific for Fas^{lpr}, 5′-CAAATTTTATTGTTGCGAC-3′.

Flow cytometry analysis

Single-cell suspensions were prepared and stained with the following Abs: FITC-conjugated anti-CD3ε mAb (145-2C11), PE-conjugated anti-CD5 mAb (53-7.3), FITC-conjugated anti-CD21 mAb (7E9) (BioLegend); PE-conjugated anti-CD23 mAb (B3B4), PE-conjugated anti-$CD72^{b+c}$ mAb (JY/93; BD Pharmingen); FITC-conjugated anti-$CD72^{a+b}$ mAb (K10.6; a kind gift from Dr. N. Tada, Tokai University, Tokyo, Japan) (26), Alexa Fluor 647–labeled anti-B220 Ab (RA3-6B2), PE-conjugated anti-CD138 mAb (c363.16A; eBioscience), and FITC-conjugated goat anti-mouse IgM (Southern Biotechnology Associates). Data was collected by a FACSCalibur (BD Biosciences) or a CyAn ADP (DakoCytomation) and analyzed using the FlowJo software (Tree Star) or Summit software (DakoCytomation), respectively.

ELISAs

Serum levels of total IgG were measured by standard sandwich ELISA. Titers of IgG Ab to dsDNA, ssDNA, and chromatin were measured by ELISAs as described previously (27). Briefly, ELISA plates were coated with 10 μg/ml dsDNA, 10 μg/ml ssDNA, or 4 μg/ml chromatin. After blocking with 0.5% BSA in PBS, 50 μl diluted serum samples were added and incubated for 60 min at room temperature. Plates were then washed and incubated with alkaline phosphatase–conjugated goat anti-mouse IgG Ab (Southern Biotechnology Associates). After washing, plates were reacted by phosphatase substrate (Sigma-Aldrich), and the absorbance at 405 nm was measured on a Vmax kinetic microplate reader (Molecular Devices). Autoantibody titers were determined using the sera pooled from (NZB × NZW) F1 mice >8 mo old as a standard.

Immunoprecipitation and Western blotting

B cells were purified from mouse spleen as described previously (28) and were stimulated with 0.2 μg/ml 4-hydroxy-3-nitrophenyl acetyl (NP)-BSA or 10 μg/ml $F(ab')_2$ fragments of goat anti-mouse IgM Ab (Jackson ImmunoResearch Laboratories). Alternatively, BAL17 cells were stimulated with 10 μg/ml $F(ab')_2$ fragments of goat anti-mouse IgM Ab at 37°C. Cells were lysed in Triton X-100 lysis buffer (1% Triton X-100, 10% glycerol, 150 mM sodium chloride, 20 mM Tris-HCl, 2 mM EDTA, 0.02% sodium azide, 10 μg/ml PMSF, and 1 mM sodium orthovanadate) and immunoprecipitated with rat anti-CD72 mAb JY/93 (BD Pharmingen) using protein G-Sepharose (Amersham Biosciences). Total cell lysates or immunoprecipitates were separated by SDS-PAGE and transferred to polyvinylidene difluoride membranes (Millipore). Membranes were incubated with goat anti-mouse IgM Ab (Southern Biotechnology Associates), rabbit anti-CD72 Ab (Santa Cruz Biotechology), or rabbit anti-p42/44 ERK Ab (Cell Signaling Technology), followed by reaction with HRP-conjugated donkey anti-goat IgG Ab (Santa Cruz Biotechnology) or HRP-conjugated goat anti-rabbit IgG Ab (Southern Biotechology Associates). Alternatively membranes were incubated with mouse anti–β-tubulin Ab TUB2.1 (Seikagaku Kogyo), followed by reaction with HRP-conjugated goat anti-mouse IgG Ab (Southern Biotechology Associates). Proteins were then visualized using ECL system (Amersham Biosciences). The intensity of protein bands was quantified using the Image J software (National Institutes of Health).

Measurement of intracellular calcium concentration

Spleen B cells were purified as described previously (29). BAL17 cells and its transfectants or purified spleen B cells (1×10^6) were incubated in culture medium containing 5 μg Fluo-4/AM (Molecular Probes) at 37°C for 30 min. Cells were stimulated with 10 μg/ml $F(ab')_2$ fragments of anti-IgM Ab or 0.2 μg/ml NP-BSA, and fluorescence was continuously measured by an FACSCalibur (BD Bioscience) for a total of 300 s.

Measurement of cell proliferation by CFSE dilution

Spleen B cells were purified as described previously (28) and labeled with 5 μM CFSE (Molecular Probes). The purity of purified cells was determined by flow cytometry using anti-B220 Ab staining (purity >93%). Cells (2×10^5/ well) were then seeded into 96-well plate and cultured in RPMI 1640 medium supplemented with 10% FCS, 50 μM 2-ME, 1 mM L-glutamine, and 100 U penicillin/streptomycin with or without 10 μg/ml anti-CD40 Ab (FGK45) (30), 10 μg/ml $F(ab')_2$ fragment of goat anti-mouse IgM Ab (Jackson ImmunoResearch Laboratories), or 10 ng/ml CpG oligomer (ODN 1668) (31) at 37°C for 72 h. The fluorescence of CFSE was measured by a CyAn ADP (DakoCytomation).

Histopathological and immunohistochemical analysis

Mice were sacrificed, and tissues were fixed in neutral buffered formalin and embedded in paraffin according to standard practices. Tissue sections (5 μm) were stained with either H&E or periodic acid–Schiff and hematoxylin (PASH). Glomerular damages were scored as described previously (32). For immunohistochemical analysis, portions of kidney were embedded in Tissue-Tek OCT compound (Sakura) and snap frozen in liquid nitrogen. Cryostat sections (7-μm thickness) were mounted onto slide glass. The sections were incubated with blocking buffer (PBS containing 0.5% BSA and 0.05% sodium azide) for 30 min and stained with FITC-conjugated anti-mouse IgG Ab (Cappel) or FITC-conjugated anti-mouse C3 Ab (Cappel) at room temperature for 1 h. Sections were analyzed using a laser-scanning microscope Leica DMI6000B (Leica Microsystems).

Detection of proteinuria

The protein level of mouse urine was semiquantitatively analyzed as described previously (33).

Statistical analysis

The data are presented as the means ± SEM, and all statistical analyses were performed using GraphPad Prism 5.0 software (GraphPad). The p values were calculated with the two-tailed Student t test (*$p < 0.05$, **$p < 0.01$, ***$p < 0.001$).

Results

Spontaneous development of lupus-like disease in B6.CD72^c/lpr congenic mice

B6/lpr and C3H /lpr mice are reported to show no or only a mild autoimmune disease (8, 9), whereas AKR/lpr and MRL/lpr mice develop moderate and severe lupus-like disease, respectively, suggesting that some genes carried by AKR and MRL mice are required for *Fas*^{lpr}-induced autoimmune disease. To address whether such a gene is located in the *Cd72*^{c} locus carried by both AKR and MRL, we generated B6.CD72^c congenic mice carrying the MRL-derived *Cd72*^{c} haplotype by selective backcrossing of the F1 hybrid between B6 carrying *Cd72*^{b} and MRL mice to B6 mice for 11 generations. Microsatellite marker analysis revealed that B6.CD72^c mice carry an MRL/lpr-derived interval on chromosome 4 containing the *Cd72*^{c} locus (Supplemental Fig. 1A). We then generated B6.CD72^c/lpr mice by crossing B6.CD72^c mice with B6/lpr mice. B6.CD72^c/lpr mice at 12 mo of age showed marked splenomegaly (Fig. 1A) and moderate lymphadenopathy (data not shown) compared with B6/lpr mice, whereas the spleen weight in B6.CD72^c mice was similar to that in B6 mice. Flow cytometry analysis revealed that percentages of T cells and B cells in both spleen and lymph nodes (LNs) of B6.CD72^c mice were

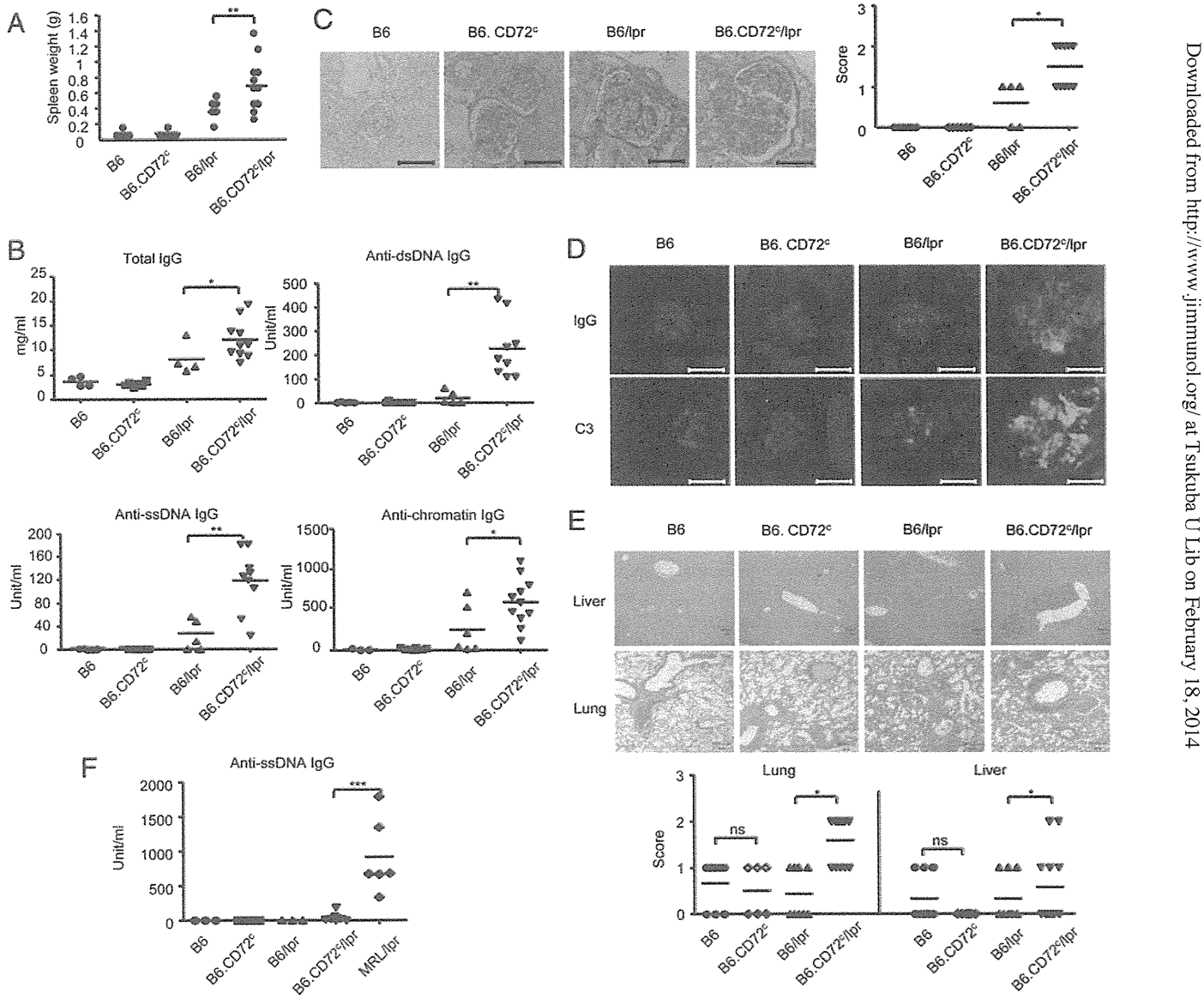

FIGURE 1. Lupus-like disease in B6.CD72^c /lpr congenic mice. (**A–E**) One-year-old female B6, B6.CD72^c, B6/lpr, and B6.CD72^c/lpr mice (n = 6–11) were analyzed. (A) Spleen weight. (B) Concentrations of total IgG and titers of indicated autoantibodies in sera. Horizontal bars represent mean values. For determining autoantibody titers, pooled sera from >8-mo-old (NZB × NZW) F1 mice are used as a standard (1000 U/ml). (C) PASH staining of glomeruli. Severity of glomerular damage was scored as described previously (32). Grade 0, no involvement; grades 1, 2, and 3, changes in 0–25%, 25–50%, and 50–75% of total glomeruli, respectively; grade 4, sclerosis or crescent formation in >90% of glomeruli. Scale bars, 50 μM. (D) Immunohistochemical analyses for IgG and C3 in glomeruli. Scale bars, 50 μM. (E) H&E staining of liver and lung. Representative data of more than five mice in each genotype are shown (original magnification ×100). Severity of the disease was scored according to the degree of lymphocyte infiltration. Grade 0, no lymphocyte infiltration; grade 1, moderate lymphocyte infiltration; and grade 2, severe lymphocyte infiltration. (**F**) Serum titer of anti-ssDNA IgG. Six-month-old female B6, B6.CD72^c, B6/lpr, B6.CD72^c/lpr, and MRL/lpr mice were analyzed (n = 3–10). *$p < 0.05$, **$p < 0.005$, ***$p < 0.001$.

similar to those of B6 mice (Table I). In contrast, B6.CD72^c/lpr mice showed marked reduction in the percentage of B cells and increase in the percentage of T cells compared with B6/lpr mice. The percentage of B220$^+$CD3$^+$ lpr T cells in B6.CD72^c/lpr mice was not increased compared with B6/lpr mice. Thus, introduction of the interval of chromosome 4 containing *Cd72*^{c} locus induced marked splenomegaly and altered T cell to B cell ratio in B6/lpr but not B6 mice, suggesting that the chromosomal interval containing *Cd72*^{c} locus does not modulate immune homeostasis by itself, but does so in the presence of *Fas*^{lpr} mutation.

Next we examined development of autoimmune disease in B6.CD72^c/lpr mice. Sera from 12-mo-old B6.CD72^c/lpr mice contained a much larger amount of IgG autoantibodies such as anti-dsDNA, anti-ssDNA, and anti-chromatin Abs compared with B6/lpr mice (Fig. 1B). Histopathological and immunohistological analysis of kidney revealed that B6.CD72^c/lpr mice developed more severe glomerular lesions with more prominent immune complex deposition compared with B6/lpr mice (Fig. 1C, 1D). Moreover, B6.CD72^c/lpr mice showed severe cell infiltration in lung and liver, whereas cell infiltration in these organs was mild in B6/lpr mice (Fig. 1E). In contrast, B6.CD72^c mice did not show any pathological findings including kidney, lung, and liver. Thus, the chromosomal interval containing *Cd72*^{c} carries a modifier gene that regulates *Fas*^{lpr}-induced autoimmune disease.

To compare the autoimmune disease in B6.CD72^c/lpr mice to that in MRL/lpr mice, we examined autoantibody production in 6-mo-old B6.CD72^c/lpr mice and MRL/lpr mice because MRL/lpr mice do not survive until 12 mo old. The titer of serum anti-DNA IgG in B6.CD72^c/lpr mice was significantly lower than that in MRL/lpr mice (Fig. 1F). Thus, MRL loci other than the *Cd72*^{c} locus are also involved in the development of severe autoimmune disease in MLR/lpr mice.

Reduced severity in autoimmune disease in MRL.CD72^b/lpr congenic mice

To further address whether *Cd72*^{c} locus regulates autoimmune disease in MRL/lpr mice, we generated MRL.CD72^b/lpr congenic mice by selective backcrossing of the F1 hybrid between MRL/lpr and B6 (*Cd72*^{b}) mice to MRL/lpr mice for 12 generations. Analysis with microsatellite markers demonstrated that a B6-derived interval on chromosome 4 containing the *Cd72* locus was introduced into MRL.CD72^b/lpr mice (Supplemental Fig. 1B). We analyzed 6-mo-old female MRL.CD72^b/lpr mice and age-matched female MRL/lpr mice. Compared to MRL/lpr mice, spleen weight (Fig. 2A), the percentage of lpr T cells in spleen (Fig. 2B), and the serum titer of anti-dsDNA and anti-ssDNA IgG (Fig. 2C) were markedly reduced in MRL.CD72^b/lpr mice. Although histological score on renal disease based on the percentage of the affected glomeruli was not much improved in MRL.CD72^b/lpr mice (Fig. 2D), these mice showed smaller glomerular size (Fig. 2E), reduced immune complex deposition (Fig. 2F), and reduced urine protein level (Fig. 2G), suggesting improvement of renal disease in MRL/lpr mice by replacing the chromosomal interval including *Cd72* locus by the B6-derived interval. Taken together, the chromosomal interval including *Cd72*^{c} plays a role in development of autoimmune disease in MRL/lpr mice, especially in expansion of lpr T cells and autoantibody production.

Augmented BCR signaling and B cell proliferation in B cells carrying CD72^c

To elucidate whether CD72^c is functionally distinct from CD72^b, we crossed B6.CD72^c mice with the QM mice on a B6 background expressing CD72^b to generate QM. CD72^c mice. As almost all B cells from QM mice express BCR reactive to hapten NP due to their expression of knocked-in VH17.2.25 and λ L chain (25), we ligated BCR in spleen B cells from QM mice and QM. CD72^c mice using an Ag NP-conjugated BSA and examined BCR signaling by analyzing calcium mobilization and phosphorylation of ERK. Although the Ca^{2+} response in QM.CD72^c B cells was similar to that in QM B cells (Fig. 3A), QM.CD72^c B cells showed augmented ERK phosphorylation compared with QM B cells (Fig. 3B).

Next, we addressed proliferative response of *Cd72*^{c}-carrying B cells to various stimuli by CFSE dilution assay. When purified spleen B cells from B6 and B6.CD72^c mice were stimulated with CpG oligomers or anti-CD40 Ab, percentage of proliferated cells were significantly higher in B6.CD72^c cells than in B6 B cells (Fig. 3C). Percentage of divided cells after anti-IgM stimulation was not increased in B6.CD72^c B cells compared with B6 B cells probably because B6 B cells fully proliferated to this stimulation. Thus, Ag-induced ERK activation and proliferative response to CpG and anti-CD40 Ab were augmented in B6.CD72^c B cells, suggesting that CD72^c negatively regulates B cell activation less efficiently than CD72^b does, although the possibility that the other

Table I. Flow cytometry analysis of spleen and LN cells from B6, B6.CD72^c, B6/lpr, and B6.CD72^c/lpr mice

Tissue	Cell Population	B6	B6.CD72^c	B6/lpr	B6.CD72^c/lpr
Spleen	Total cell number ($\times 10^6$)	145.0 ± 11.0	127.0 ± 9.2	320.0 ± 100.0	764.3 ± 38.9*
	Phenotype (%)[a]				
	B220$^+$CD3$^-$ (B cells)	55.9 ± 3.1	56.0 ± 6.9	46.4 ± 3.9	18.1 ± 5.8**
	($\times 10^6$)[b]	(80.1 ± 4.8)	(69.2 ± 11.9)	(133.4 ± 38.3)	(137.6 ± 47.6)
	CD3$^+$B220$^-$ (T cells)	25.5 ± 3.2	20.3 ± 6.3	24.3 ± 3.4	40.5 ± 4.5*
	($\times 10^6$)	(37.9 ± 6.4)	(24.3 ± 9.9)	(89.2 ± 35.4)	(315.8 ± 43.4)**
	B220$^-$CD3$^-$	16.8 ± 1.9	21.4 ± 8.1	22.5 ± 4.4	34.5 ± 10.1*
	($\times 10^6$)	(25.3 ± 4.6)	(27.6 ± 9.6)	(84.0 ± 30.9)	(255.4 ± 75.8)**
	B220$^+$CD3$^+$ (lpr T cells)	1.6 ± 0.1	1.2 ± 0.4	6.7 ± 2.3	7.3 ± 2.7
	($\times 10^6$)	(3.4 ± 1.3)	(1.6 ± 0.6)	(13.4 ± 3.7)	(55.5 ± 21.2)*
LN	Phenotype (%)[b]				
	B220$^+$CD3$^-$ (B cells)	52.9 ± 6.3	44.2 ± 6.9	43.3 ± 3.0	17.9 ± 7.5*
	CD3$^+$B220$^-$ (T cells)	40.2 ± 6.3	45.1 ± 9.9	24.7 ± 4.1	52.0 ± 8.2*
	B220$^-$CD3$^-$	5.8 ± 1.1	9.4 ± 3.7	4.1 ± 2.6	1.9 ± 0.5
	B220$^+$CD3$^+$ (lpr T cells)	0.9 ± 0.2	1.1 ± 0.3	27.1 ± 1.3	27.3 ± 3.0

Data were obtained from 12–14-mo-old mice and are expressed as mean ± SEM (n = 6 to 7).

[a]Percentages of cells expressing the indicated surface markers in total lymphocyte-gated cells from spleen and LN.

[b]Absolute cell numbers are indicated in parentheses. Statistical significance was calculated between B6 and B6.CD72^c mice and between B6/lpr and B6/lpr.CD72^c mice.

*$p < 0.05$, **$p < 0.01$.

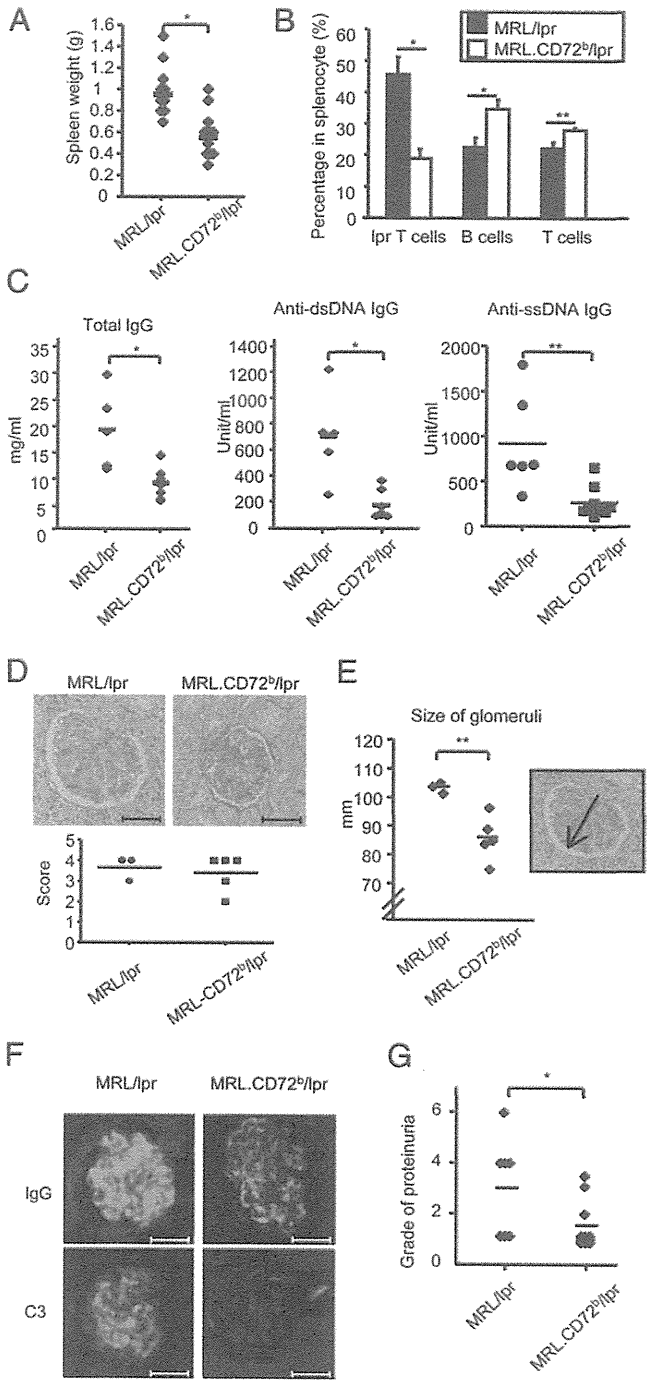

FIGURE 2. Reduced severity of autoimmune disease in MRL.CD72^b/lpr mice. Female MRL/lpr and MRL.CD72^b/lpr mice at 6 mo old were analyzed. (**A**) Spleen weights (n = 10–16). (**B**) Percentages of lpr T cells ($B220^+CD3^+$), B cells ($B220^+CD3^-$), and T cells ($B220^-CD3^+$) in total lymphocyte-gated splenocytes were measured by flow cytometry (n = 3). (**C**) Concentrations of total IgG and titers of anti-dsDNA and anti-ssDNA IgG in sera were measured by ELISA (n = 5–9). For determining autoantibody titers, pooled sera from >8-mo-old (NZB × NZW) F1 mice are used as a standard (1000 U/ml). (**D**) PASH staining of glomeruli (n = 3–5). Severity of glomerular damage was scored as in the legend to Fig. 1C. Glomeruli are shown at the same magnification. Scale bars, 50 μM. (**E**) Size of glomeruli (n = 3–5). The diameter of glomeruli from vascular pole of five randomly selected glomeruli was measured on PASH-stained sections of kidneys (original magnification ×400). Each dot represents the mean value of the glomerular diameter for each mouse. (**F**) Immunohistochemical analysis of glomeruli for IgG and C3. Representative data of more than three mice in each genotype are shown. Scale bars, 50 μM. (**G**) Urine protein level. Urine was spotted on filter paper, and the protein level was semiquantitatively measured (n = 7–12). The grade of proteinuria was defined as follows: grade 6, equivalent to 30 mg/ml BSA; grade 5, 10 mg/ml BSA; grade 4, 3.3 mg/ml BSA; grade 3, 1.1 mg/ml BSA; grade 2, 0.74 mg/ml BSA; and grade 1, 0.37 mg/ml BSA. *$p < 0.05$, **$p < 0.005$.

genes in the MRL-derived interval in B6.CD72^c mice regulate B cell activation is not excluded.

To directly demonstrate that CD72^c poorly regulates BCR signaling, we transduced CD72^c and CD72^a, the latter of which is highly homologous to CD72^b, to the mouse B cell line BAL17 and examined their capacity to regulate BCR signaling. As BAL17 cells express endogenous CD72^b (34), we examined the expression of the transduced CD72^a and CD72^c by flow cytometry using anti-CD72 mAbs reactive to CD72^a and CD72^b and that reactive to CD72^b and CD72^c, respectively. The expression level of CD72 in BAL17-CD72^a transfectant and BAL17-CD72^c transfectant are 1.74 and 3.58 times higher than parent BAL17 cells, respectively (Fig. 3D). We are not able to exclude the possibility that these anti-CD72 Abs react to different CD72 allelic forms with different efficiency or the possibility that transduced CD72 affects expression of endogenous CD72 or forms a heterodimer with endogenous CD72. Nonetheless, our result on flow cytometry suggests that CD72^c expression in BAL17-CD72^c cells is higher than CD72^a expression in BAL17-CD72^a cells. We then ligated BCR on BAL17 transfectants using anti-IgM Ab and analyzed calcium mobilization and ERK phosphorylation. Both calcium mobilization and ERK phosphorylation induced by BCR ligation were reduced in BAL17-CD72^a transfectant compared with control transfectant (Fig. 3E, 3F), indicating that CD72^a negatively regulates BCR signaling in agreement with previous findings (14). In contrast, CD72^c expression reduced both calcium mobilization and ERK phosphorylation only marginally if any (Fig. 3E, 3F), although the CD72 expression level in CD72^c transfectant is higher than that in CD72^a transfectant. Thus, CD72^c regulates BCR signaling less efficiently than CD72^a in both primary B cells and BAL17 cells.

CD72^c differs from CD72^a or CD72^b at the extracellular part but not the cytoplasmic region including ITIM. To address how the extracellular part of CD72^c reduces its negative-regulatory activity on B cell activation, we examined association of CD72 to BCR. When we immunoprecipitated CD72^b and CD72^c from lysates of B6 and B6.CD72^c B cells, respectively, CD72^b coprecipitated more IgM than CD72^c did (Fig. 3G). This result suggests that CD72^c associates with BCR less strongly than CD72^b does, although we are not able to exclude the possibility that anti-CD72 Abs differently react to the different CD72 allelic forms, resulting in different immunoprecipitation and detection efficiency depending on the allelic forms. Taken together, CD72^c regulates B cell signaling and B cell activation inefficiently probably due to its weak association to BCR.

CD72 deficiency causes severe autoimmune disease in the presence of Fas^{lpr} mutation

As CD72^c regulates BCR signaling less efficiently than CD72^a, we next addressed whether CD72 deficiency induces severe autoimmune disease in the presence of the Fas^{lpr} gene by generating $Cd72^{-/-}$ mice on a B6 background (Supplemental Fig. 2). When we examined signaling properties of $Cd72^{-/-}$ B6 B cells, BCR ligation–induced ERK phosphorylation was augmented compared with that in wild-type B6 B cells expressing CD72^b (Fig. 4A), whereas calcium signaling in $Cd72^{-/-}$ B cells was similar to that

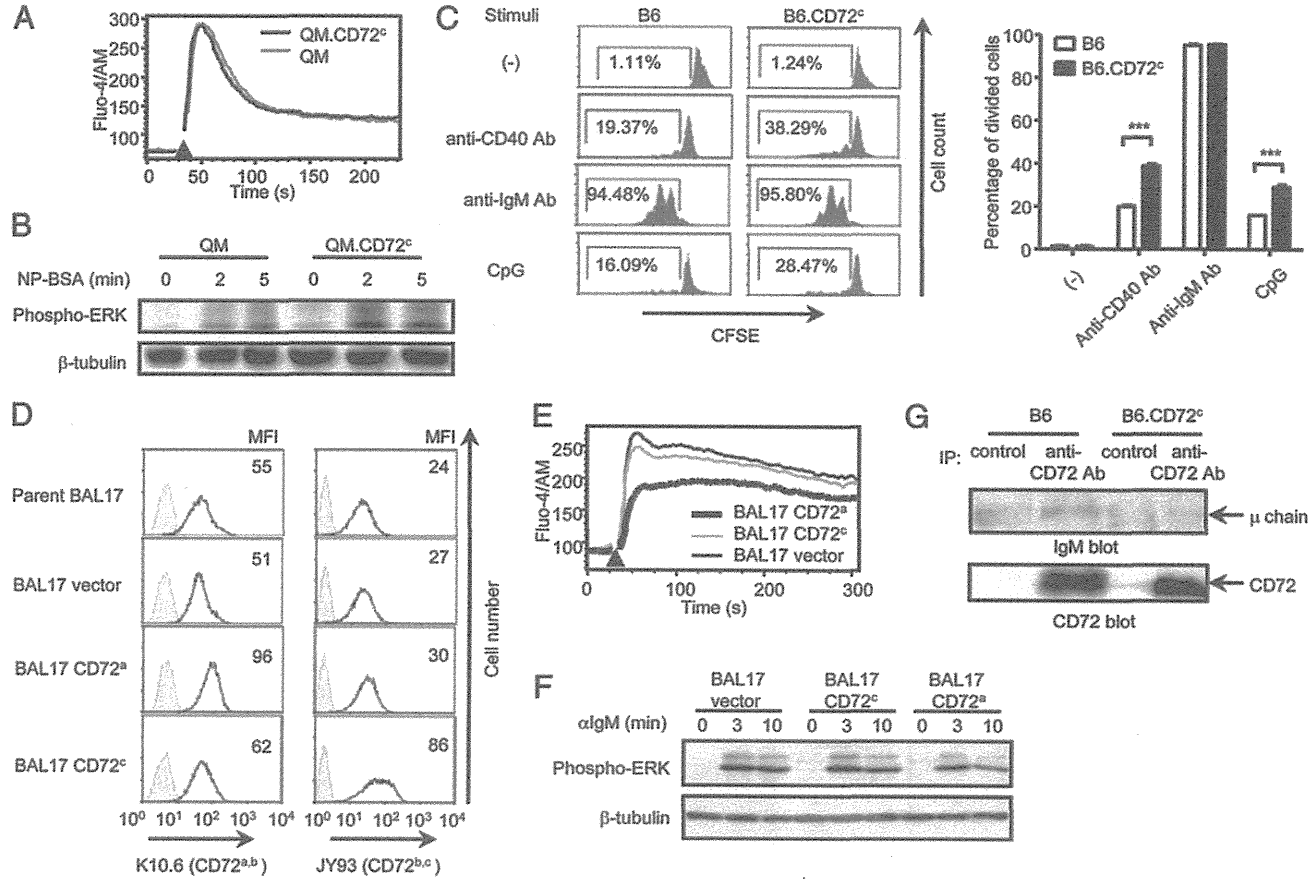

FIGURE 3. $CD72^c$ is a poor negative regulator of BCR signaling and B cell activation. Spleen B cells were purified from 8–12-wk-old QM and QM.$CD72^c$ mice. Fluo-4/AM-loaded (**A**) or untreated (**B**) cells were stimulated with 0.2 μg/ml NP-BSA. Intracellular free calcium ion level was measured by flow cytometry (A). The arrowhead indicates the time point when NP-BSA was added. Alternatively, total cell lysates were analyzed for phosphorylation of ERK by Western blotting (B). The same membrane was reprobed with anti–β-tubulin Ab to ensure equal loading. Representative data of three experiments are shown. (**C**) Purified spleen B cells from B6 or B6.$CD72^c$ mice were labeled with CFSE and cultured with indicated reagents for 72 h. CFSE fluorescence was analyzed by flow cytometry. The percentages of proliferated cells are indicated (*left panel*). Mean ± SD of triplicate is shown (*right panel*). Data are representative of three independent experiments. (**D**) CD72 expression in indicated BAL17 transfectants were analyzed by flow cytometry using anti-CD72 Abs K10.6 reactive to $CD72^a$ and $CD72^b$ and JY/93 reactive to $CD72^b$ and $CD72^c$. Mean fluorescence intensity (MFI) is indicated. Unstained cells were used as negative controls (shaded histograms). Fluo-4/AM–loaded (**E**) or untreated (**F**) BAL17 transfectants were stimulated with 10 μg/ml anti-IgM Ab. Calcium ion concentration was analyzed by flow cytometry (E). The arrowhead indicates the time point when anti-IgM Ab was added. Representative data of five experiments are shown. Total cell lysates were analyzed for phosphorylation of ERK by Western blotting (F). The same membrane was reprobed with anti–β-tubulin Ab to ensure equal loading. Representative data of three experiments are shown. (**G**) Total cell lysates of purified spleen B cells from B6 and B6.$CD72^c$ mice were immunoprecipitated (IP) with anti-CD72 or control Ab and analyzed by Western blotting using anti-IgM and anti-CD72 Abs. Representative data of three experiments are shown. $***p < 0.001$.

in wild-type B6 B cells (Fig. 4B). Thus, CD72 appears to efficiently regulate BCR ligation–induced ERK phosphorylation but not calcium signaling in agreement with our results in QM.$CD72^c$ B cells and BAL17 transfectants (Fig. 3). Proliferative response to CpG and anti-CD40 Ab was augmented in $Cd72^{-/-}$ B cells compared with wild-type B6 B cells (Fig. 4*C*), as is the case for B6.$CD72^c$ B cells. Thus, signaling and proliferative properties of $Cd72^{-/-}$ B cells are similar to those of $Cd72^c$-carrying B cells.

We then bred $Cd72^{-/-}$ mice with B6/lpr mice and analyzed 6-mo-old female $Cd72^{-/-}$ B6/lpr mice. These mice showed severe splenomegaly (Fig. 4D) and lymphadenopathy (data not shown) and marked expansion of lpr T cells in spleen, LNs, and peritoneal cavity (peritoneal exudate cells [PEC]) (Tables II, III), whereas expansion of lpr T cells is mild in B6/lpr mice. As is the case for B6.$CD72^c$/lpr mice, percentages of T cells and B cells were increased and decreased, respectively, in $Cd72^{-/-}$ B6/lpr mice (Table II). In contrast, $Cd72^{-/-}$ mice showed mild splenomegaly but no distorted proportions of T and B cells. Thus, CD72 deficiency induces marked splenomegaly synergistically with the Fas^{lpr} gene and accelerates expansion of lpr T cells.

Although the serum IgG level in $Cd72^{-/-}$ B6 and $Cd72^{-/-}$ B6/lpr mice at 6 mo of age were comparable to that in age-matched $Cd72^{+/+}$ B6 mice, the high titer of anti-chromatin IgG was produced in both $Cd72^{-/-}$ and $Cd72^{-/-}$ B6/lpr mice (Fig. 4E). Although the titers of anti-dsDNA and anti-ssDNA IgG were significantly increased in $Cd72^{-/-}$ B6 mice compared with $Cd72^{+/+}$ B6 mice, the titers of these autoantibodies were markedly higher in $Cd72^{-/-}$ B6/lpr mice than in $Cd72^{-/-}$ B6 mice (Fig. 4E), suggesting that CD72 deficiency induces production of a large amount of anti-DNA Abs in the presence of the Fas^{lpr} gene. Histopathological analysis revealed development of glomerulonephritis with immune complex deposition (Fig. 4F, 4G) and cell infiltration in lung (Fig. 4H) in $Cd72^{-/-}$ B6 mice, which are consistent with the previous report (35). $Cd72^{-/-}$ B6/lpr mice developed more severe glomerulonephritis and cell infiltration in lung and liver than $Cd72^{-/-}$ B6 or B6/lpr mice, suggesting that CD72 deficiency induces development of autoimmune glomeru-

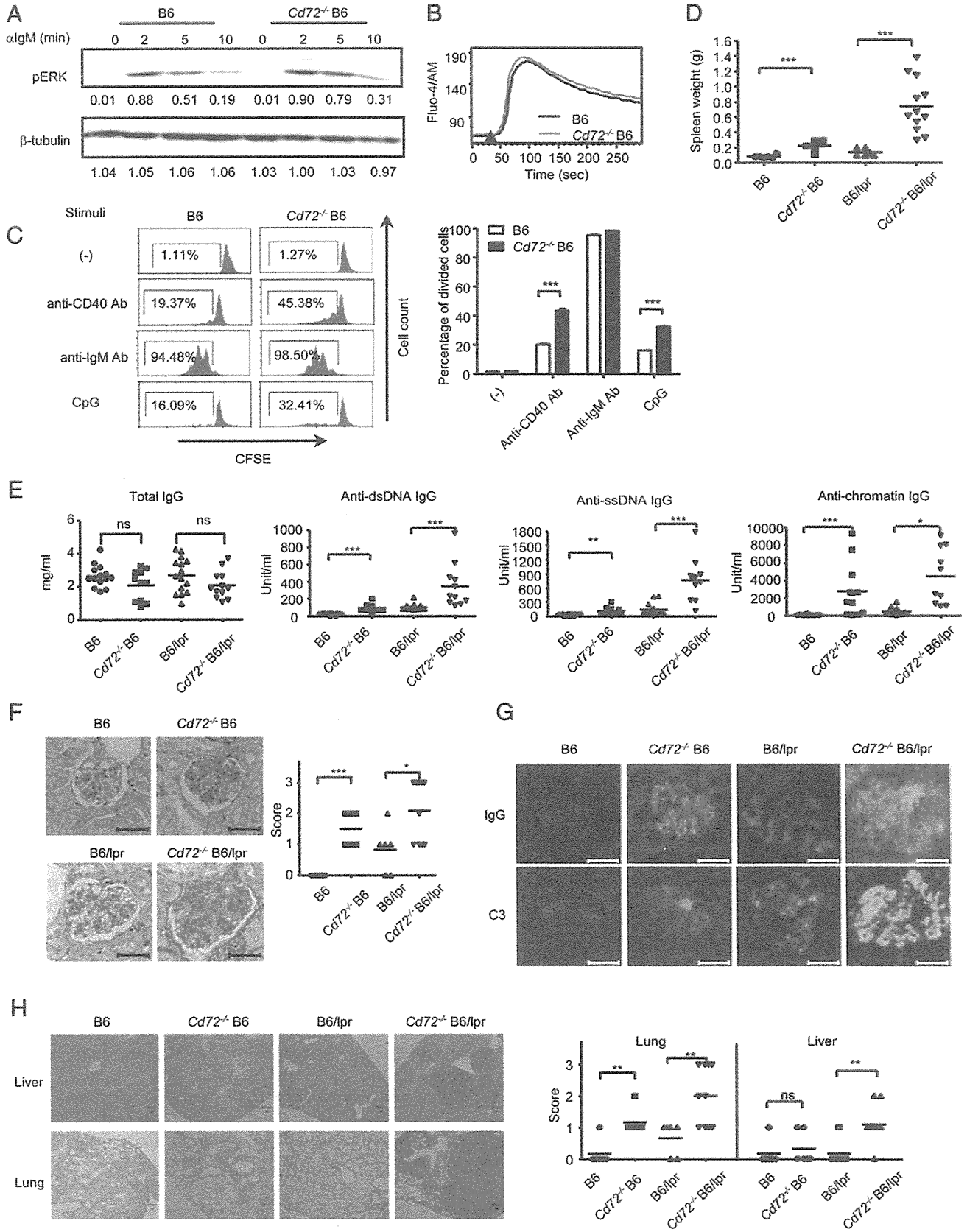

FIGURE 4. Severe autoimmune disease in *Cd72*$^{-/-}$ B6/lpr mice. (**A** and **B**) Spleen B cells were purified from 8–12-wk-old B6 and *Cd72*$^{-/-}$ B6 mice. Total cell lysates were analyzed for phosphorylation of ERK by Western blotting (A). The same membrane was reprobed with anti–β-tubulin Ab to ensure equal loading. The intensity of the protein bands was quantified, and the relative amounts of phosphorylated ERK and β-tubulin are indicated. Representative data of three experiments are shown. Alternatively, Fluo-4/AM–loaded cells were stimulated with 10 μg/ml anti-IgM Ab (B). Intracellular free calcium ion level was measured by flow cytometry. The arrowhead indicates the time point when anti-IgM Ab was added. (**C**) Purified B cells from B6 and *Cd72*$^{-/-}$ B6 mice were labeled with CFSE and cultured with indicated reagents for 72 h. CFSE fluorescence was analyzed by (*Figure legend continues*)

Table II. Flow cytometry analysis of spleen cells from B6, *Cd72*$^{-/-}$ B6, B6/lpr, and *Cd72*$^{-/-}$ B6/lpr mice

Cell Population	B6	*Cd72*$^{-/-}$ B6	B6/lpr	*Cd72*$^{-/-}$ B6/lpr
Total cell number ($\times 10^6$)	98.8 ± 9.3	160.2 ± 15.4	121.6 ± 12.4	308.8 ± 92.8
Phenotype (%)[a]				
$B220^+CD3^-$ (B cells)	45.6 ± 2.2	40.0 ± 2.4	55.1 ± 1.3	21.6 ± 3.6**
($\times 10^6$)[b]	(44.5 ± 3.9)	(63.2 ± 6.2)	(66.9 ± 6.5)	(54.4 ± 6.6)
$CD3^+B220^-$ (T cells)	41.4 ± 2.7	41.7 ± 1.2	19.4 ± 1.2	31.0 ± 4.2*
($\times 10^6$)	(41.3 ± 5.3)	(66.3 ± 5.6)	(23.8 ± 3.6)	(108.7 ± 49.6)*
$B220^-CD3^-$	12.1 ± 1.4	16.3 ± 2.4	8.0 ± 1.0	16.0 ± 2.5*
($\times 10^6$)	(12.0 ± 1.6)	(27.3 ± 5.5)	(9.6 ± 1.2)	(41.9 ± 4.9)**
$B220^+CD3^+$ (lpr T cells)	0.9 ± 0.1	2.0 ± 0.5	17.5 ± 1.2	31.3 ± 3.7**
($\times 10^6$)	(0.9 ± 0.2)	(3.4 ± 1.0)	(21.3 ± 2.6)	(103.8 ± 40.5)*
Phenotype of $B220^+$ B cells (%)[b]				
$CD21^{\pm}CD23^{hi}$ (FO B cells)	76.1 ± 2.1	52.6 ± 3.1*	46.3 ± 1.4	15.8 ± 5.0***
$CD21^{hi}CD23^{\pm}$ (MZ B cells)	11.0 ± 0.9	7.2 ± 0.7*	10.8 ± 0.9	0.6 ± 0.3***

Data were obtained from 6-mo-old mice and are expressed as mean ± SEM (n = 5 to 6). Statistical significance was calculated between B6 and *Cd72*$^{-/-}$ B6 mice and between B6/lpr and *Cd72*$^{-/-}$ B6/lpr mice.

[a]Percentages of cells expressing the indicated surface markers in lymphocyte-gated cells.

[b]Absolute cell numbers are indicated in parentheses.

*$p < 0.05$, **$p < 0.01$, ***$p < 0.001$.

FO, Follicular; MZ, marginal zone.

lonephritis and cell infiltration in lung and liver synergistically with the *Fas*^{lpr} gene.

Discussion

Autoimmune disease caused by *Fas*^{lpr} depends on the genetic background of mouse strains. In this study, we demonstrate that introduction of the MRL-derived chromosomal interval containing *Cd72*^{c} into B6 mice did not cause any disease but markedly enhanced severity of autoimmune disease in B6/lpr mice. This result clearly demonstrates that this locus contains a modifier gene that regulates *Fas*^{lpr}-induced autoimmune disease. Conversely, introduction of the B6-derived interval containing *Cd72*^{b} reduced the severity of the disease in MRL/lpr mice further support the crucial role of this locus in regulation of *Fas*^{lpr}-induced autoimmune disease. We also demonstrated that CD72^c is hypofunctional in regulating BCR signaling and B cell activation and that CD72 deficiency induces severe autoimmune disease in the presence of *Fas*^{lpr}. Thus, in B6.CD72^c/lpr mice, the hypofunctional *Cd72*^{c} allele but not other genes in the MRL-derived chromosomal interval appears to be responsible for induction of severe autoimmune disease, and *Cd72*^{c} is a modifier gene that regulates *Fas*^{lpr}-induced autoimmune disease.

Our finding on the role of *Cd72*^{c} in development of autoimmune disease is also supported by the finding by Oishi et al. (36). They generated MRL/lpr mice carrying a BAC transgene encoding *Cd72*^{b} and a mutant BAC in which exon 8 encoding a part of the extracellular region of *Cd72* was replaced by the exon 8 derived from *Cd72*^{c}. The *Cd72*^{b}-containing BAC but not the mutant BAC markedly reduced BCR signaling and severity of the autoimmune disease in MRL/lpr mice, clearly demonstrating distinct functional activity of CD72^c and its role in development of autoimmune disease in MRL/lpr mice, in agreement with our finding. Previously, Li et al. (35) demonstrated that *Cd72*$^{-/-}$ mice spontaneously develop autoimmune manifestations including glomerulonephritis and inflammatory infiltration of the lung and salivary glands at 1 y of age, and we confirmed this finding in the independently established *Cd72*$^{-/-}$ mouse line (Fig. 4). Thus, CD72 deficiency but not *Cd72*^{c} causes mild lupus-like disease by itself. *Cd72*^{c} may not cause autoimmune disease by itself as it probably retains its regulatory activity to some extent. Thus, a hypofunctional allele of a gene that is crucial for preventing autoimmune disease can play a role as a modifier gene.

An old study demonstrated that the *Fas*^{lpr} locus induces autoimmune disease in mice with AKR but not C3H or B6 backgrounds (8). Because AKR as well as MRL carries *Cd72*^{c}, *Cd72*^{c} may be a modifier gene involved in the development of autoimmune disease in AKR/lpr as well as MRL/lpr mice. In human, mutations of *Fas* cause autoimmune lymphoproliferative syndrome (ALPS), in which penetrance is variable among families (6, 7, 37). As there is a functional difference between human *CD72* haplotypes (38, 39), CD72 polymorphism may play a crucial role in the regulation of penetrance and disease manifestations in ALPS. Modifier genes are extensively studied in various diseases including cystic fibrosis, arrhythmia, and cancer because modifier genes extensively regulate penetrance, severity, and manifestations of these diseases (1–3). Also, modifier genes can be a good target of therapy and prevention if it is difficult to correct the defect caused by disease-causing mutations. However, little is known about modifier genes that regulate autoimmune diseases. The *Yaa* gene may be another modifier gene that regulates autoimmune diseases because it is required for development of autoimmune disease in BXSB mice but does not induce autoimmune disease by itself in the B6 background (40), although *Yaa* is naturally found only in BXSB mice. As most cases of autoimmune diseases appear to involve multiple genes, all of which contribute to a minor component (41), it may not be straightforward to dis-

flow cytometry. The percentages of proliferated cells are indicated (*left panel*). Mean ± SD of triplicate is shown (*right panel*). Data are representative of three independent experiments. ***$p < 0.0001$. (**D–H**) Female wild-type B6, *Cd72*$^{-/-}$ B6, B6/lpr, and *Cd72*$^{-/-}$ B6/lpr mice at 6 mo old were analyzed. (D) Spleen weight (n = 6–12). (E) Concentrations of total IgG and titers of anti-dsDNA, anti-ssDNA, and anti-chromatin IgG in sera were determined by ELISA. For determining autoantibody titers, pooled sera from >8-mo-old (NZB × NZW) F1 mice are used as a standard (1000 U/ml). Horizontal bars represent mean values (n = 10–14). (F) PASH staining of glomeruli. Severity of glomerular damage was scored as in the legend to Fig. 1C. Scale bars, 50 μM. (G) Immunohistochemical analyses for IgG and C3 in glomeruli. Scale bars, 50 μM. (H) H&E staining of liver and lung (original magnification ×100). Severity of the disease was scored as in the legend to Fig. 1E. Representative data of more than six mice in each genotype are shown. *$p < 0.05$, **$p < 0.005$, ***$p < 0.001$.

Table III. Flow cytometric analysis of LN, bone marrow, and PEC from B6, *Cd72*$^{-/-}$ B6, B6/lpr, and *Cd72*$^{-/-}$ B6/lpr mice

Tissue	Cell Population	B6	*Cd72*$^{-/-}$ B6	B6/lpr	*Cd72*$^{-/-}$ B6/lpr
LN	B220$^+$CD3$^-$ (B cells)	28.0 ± 2.1	29.2 ± 2.2	42.2 ± 3.6	13.6 ± 4.2**
	CD3$^+$B220$^-$ (T cells)	69.3 ± 2.2	64.8 ± 2.0	10.9 ± 1.0	26.1 ± 2.8**
	B220$^+$CD3$^+$ (lpr T cells)	0.4 ± 0.1	0.6 ± 0.1	42.0 ± 4.3	57.7 ± 2.2*
BM	B220$^+$IgM$^-$ (pre-B cells)	10.8 ± 1.1	19.5 ± 2.2*	15.4 ± 2.5	8.3 ± 1.6*
	B220^{low}IgM^{low} (immature B cells)	6.5 ± 0.8	6.6 ± 0.3	5.0 ± 0.7	2.2 ± 0.4*
	B220$^+$IgM^{high} (transitional B cells)	2.7 ± 0.5	1.5 ± 0.3	1.8 ± 0.3	0.7 ± 0.4*
	B220^{high}IgM^{low} (mature B cells)	6.5 ± 0.8	4.9 ± 0.6	3.4 ± 1.2	2.6 ± 0.6
PEC	IgM^{high}CD5$^+$ (B1-a cells)	12.2 ± 2.9	11.6 ± 3.8	3.1 ± 0.2	4.5 ± 0.1
	IgM$^-$B220$^+$CD5$^+$ (lpr T cells)	ND	ND	32.9 ± 6.6	56.0 ± 0.7*

Data were obtained from 6-mo-old mice and are expressed as mean ± SEM (n = 5 to 6). Values represent the percentages of cells expressing the indicated surface makers in total lymphocyte-gated cells from bone marrow (BM), PEC, and LN. Statistical significance was calculated between B6 and *Cd72*$^{-/-}$ B6 mice and between B6/lpr and *Cd72*$^{-/-}$ B6/lpr mice.

*$p < 0.05$, **$p < 0.001$.

ND, Not detected.

tinguish modifier genes from disease-causing genes in autoimmune diseases, except for the cases in which a single gene plays a dominant role, such as patients with ALPS and MRL/lpr mice.

In this study, the autoimmune disease in B6.CD72^c/lpr mice is less severe than that in MRL/lpr mice, indicating involvement of other MRL-derived genes in development of the severe disease. This is consistent with the previous findings on the association of other genetic loci such as the *Opn* (20) and *FcγRIIB* loci (42, 43) with development of autoimmune disease in MRL/lpr mice. Thus, multiple genes including *Fas*^{lpr} and *Cd72*^{c} are involved in development of severe autoimmune disease in MRL/lpr mice. Lack of these genes other than *Fas*^{lpr} and *Cd72*^{c} may explain why AKR/lpr develops milder autoimmune disease than MRL/lpr does. Identification of the modifier genes in the MRL background that are involved in the autoimmune disease enables us to study how these genes interact with each other and ultimately induce the autoimmune disease.

It is already well established that CD72 is a negative regulator of BCR signaling (12–16). Expression of CD72^a negatively regulates both calcium signaling and ERK phosphorylation induced by BCR ligation in BAL17 cells (Fig. 3). In contrast, *Cd72*$^{-/-}$ B cells show augmented ERK phosphorylation but no alteration in calcium signaling induced by treatment with anti-IgM Ab (Fig. 4A, 4B). However, a previous study demonstrated that BCR ligation-induced calcium response is enhanced in *Cd72*$^{-/-}$ B cells (15, 16). Thus, CD72-mediated regulation of BCR signaling depends on experimental conditions. In the current study, we demonstrated that CD72^c is hypofunctional. This property of CD72^c may cause enhanced B cell activation, which may be involved in development of autoimmune disease through augmented autoantibody production. The hypofunctional property of CD72^c may not be due to its expression efficiency on the cell surface as surface expression level of CD72^c in B6.CD72^c B cells appears to be equivalent to that of CD72^b in B6 B cells, although it is not proven if the anti-CD72 Ab used for measuring CD72 expression level detects CD72^b and CD72^c equally (Supplemental Fig. 3). In contrast, CD72^c coprecipitates BCR less efficiently than CD72^a (Fig. 3G), suggesting that interaction of CD72^c with BCR is weaker than that of CD72^a. As interaction and colocalization of inhibitory coreceptors including FcγRIIB with BCR is crucial for their inhibitory activity (44, 45), less efficient interaction of CD72^c with BCR may reduce its regulatory activity on BCR signaling. CD72^c contains several amino acid substitutions and a 7-aa deletion in the extracellular region compared with CD72^a or CD72^b, whereas the cytoplasmic region of CD72^c is identical to that of CD72^a or CD72^b (18, 19). Alterations in the extracellular region of CD72 may change its association with BCR or binding to its ligands, leading to reduction in its colocalization with BCR either directly or indirectly. Although CD100 was reported to be a ligand of CD72 (46), there might be other ligands. Thus, full elucidation of the interaction of CD72 with BCR and ligands may be crucial to understand the defect in signaling function of CD72^c and its role in development of autoimmune disease.

Acknowledgments

We thank Dr. T. Kitamura (University of Tokyo, Tokyo, Japan) for cell lines, Dr. M. Wabl (University of California, San Francisco) for QM mice, Dr. N. Tada (Tokai University, Tokyo, Japan) for reagent, Dr. M. Nose (Ehime University, Ehime Prefecture, Japan) for discussion, T. Usami (Tokyo Medical and Dental University) for technical assistance, and S.S. Devi for initial work on the generation of B6.CD72^c mice.

Disclosures

The authors have no financial conflicts of interest.

References

1. Cutting, G. R. 2005. Modifier genetics: cystic fibrosis. *Annu. Rev. Genomics Hum. Genet.* 6: 237–260.
2. Nadeau, J. H. 2001. Modifier genes in mice and humans. *Nat. Rev. Genet.* 2: 165–174.
3. Hamilton, B. A., and B. D. Yu. 2012. Modifier genes and the plasticity of genetic networks in mice. *PLoS Genet.* 8: e1002644.
4. Nagata, S. 1998. Human autoimmune lymphoproliferative syndrome, a defect in the apoptosis-inducing Fas receptor: a lesson from the mouse model. *J. Hum. Genet.* 43: 2–8.
5. Watanabe-Fukunaga, R., C. I. Brannan, N. G. Copeland, N. A. Jenkins, and S. Nagata. 1992. Lymphoproliferation disorder in mice explained by defects in Fas antigen that mediates apoptosis. *Nature* 356: 314–317.
6. Rieux-Laucat, F., F. Le Deist, C. Hivroz, I. A. Roberts, K. M. Debatin, A. Fischer, and J. P. de Villartay. 1995. Mutations in Fas associated with human lymphoproliferative syndrome and autoimmunity. *Science* 268: 1347–1349.
7. Fisher, G. H., F. J. Rosenberg, S. E. Straus, J. K. Dale, L. A. Middleton, A. Y. Lin, W. Strober, M. J. Lenardo, and J. M. Puck. 1995. Dominant interfering Fas gene mutations impair apoptosis in a human autoimmune lymphoproliferative syndrome. *Cell* 81: 935–946.
8. Kelley, V. E., and J. B. Roths. 1985. Interaction of mutant lpr gene with background strain influences renal disease. *Clin. Immunol. Immunopathol.* 37: 220–229.
9. Izui, S., V. E. Kelley, K. Masuda, H. Yoshida, J. B. Roths, and E. D. Murphy. 1984. Induction of various autoantibodies by mutant gene lpr in several strains of mice. *J. Immunol.* 133: 227–233.
10. Takahashi, S., S. Futatsugi-Yumikura, A. Fukuoka, T. Yoshimoto, K. Nakanishi, and S. Yonehara. 2013. Fas deficiency in mice with the Balb/c background induces blepharitis with allergic inflammation and hyper-IgE production in conjunction with severe autoimmune disease. *Int. Immunol.* DOI: 10.1093/intimm/dxs109.
11. Nakayama, E., I. von Hoegen, and J. R. Parnes. 1989. Sequence of the Lyb-2 B-cell differentiation antigen defines a gene superfamily of receptors with inverted membrane orientation. *Proc. Natl. Acad. Sci. USA* 86: 1352–1356.
12. Adachi, T., H. Flaswinkel, H. Yakura, M. Reth, and T. Tsubata. 1998. The B cell surface protein CD72 recruits the tyrosine phosphatase SHP-1 upon tyrosine phosphorylation. *J. Immunol.* 160: 4662–4665.
13. Wu, Y., M. J. Nadler, L. A. Brennan, G. D. Gish, J. F. Timms, N. Fusaki, J. Jongstra-Bilen, N. Tada, T. Pawson, J. Wither, et al. 1998. The B-cell trans-

membrane protein CD72 binds to and is an in vivo substrate of the protein tyrosine phosphatase SHP-1. *Curr. Biol.* 8: 1009–1017.
14. Adachi, T., C. Wakabayashi, T. Nakayama, H. Yakura, and T. Tsubata. 2000. CD72 negatively regulates signaling through the antigen receptor of B cells. *J. Immunol.* 164: 1223–1229.
15. Li, D. H., J. W. Tung, I. H. Tarner, A. L. Snow, T. Yukinari, R. Ngernmaneepothong, O. M. Martinez, and J. R. Parnes. 2006. CD72 downmodulates BCR-induced signal transduction and diminishes survival in primary mature B lymphocytes. *J. Immunol.* 176: 5321–5328.
16. Pan, C., N. Baumgarth, and J. R. Parnes. 1999. CD72-deficient mice reveal nonredundant roles of CD72 in B cell development and activation. *Immunity* 11: 495–506.
17. Tung, J. S., F. W. Shen, V. LaRegina, and E. A. Boyse. 1986. Antigenic complexity and protein-structural polymorphism in the Lyb-2 system. *Immunogenetics* 23: 208–210.
18. Robinson, W. H., H. Ying, M. C. Miceli, and J. R. Parnes. 1992. Extensive polymorphism in the extracellular domain of the mouse B cell differentiation antigen Lyb-2/CD72. *J. Immunol.* 149: 880–886.
19. Ying, H., E. Nakayama, W. H. Robinson, and J. R. Parnes. 1995. Structure of the mouse CD72 (Lyb-2) gene and its alternatively spliced transcripts. [Published erratum appears in 1995 *J. Immunol.* 155: 1637b.] *J. Immunol.* 154: 2743–2752.
20. Miyazaki, T., M. Ono, W. M. Qu, M. C. Zhang, S. Mori, S. Nakatsuru, Y. Nakamura, T. Sawasaki, Y. Endo, and M. Nose. 2005. Implication of allelic polymorphism of osteopontin in the development of lupus nephritis in MRL/lpr mice. *Eur. J. Immunol.* 35: 1510–1520.
21. Qu, W. M., T. Miyazaki, M. Terada, L. M. Lu, M. Nishihara, A. Yamada, S. Mori, Y. Nakamura, H. Ogasawara, C. Yazawa, et al. 2000. Genetic dissection of vasculitis in MRL/lpr lupus mice: a novel susceptibility locus involving the *CD72*^{c} allele. *Eur. J. Immunol.* 30: 2027–2037.
22. Nose, M. 2011. A polygene network model for the complex pathological phenotypes of collagen disease. *Pathol. Int.* 61: 619–629.
23. Kitamura, T., Y. Koshino, F. Shibata, T. Oki, H. Nakajima, T. Nosaka, and H. Kumagai. 2003. Retrovirus-mediated gene transfer and expression cloning: powerful tools in functional genomics. *Exp. Hematol.* 31: 1007–1014.
24. Onishi, M., S. Kinoshita, Y. Morikawa, A. Shibuya, J. Phillips, L. L. Lanier, D. M. Gorman, G. P. Nolan, A. Miyajima, and T. Kitamura. 1996. Applications of retrovirus-mediated expression cloning. *Exp. Hematol.* 24: 324–329.
25. Cascalho, M., A. Ma, S. Lee, L. Masat, and M. Wabl. 1996. A quasi-monoclonal mouse. *Science* 272: 1649–1652.
26. Tada, N., S. Kimura, Y. Liu, B. A. Taylor, and U. Hämmerling. 1981. Ly-m19: the Lyb-2 region of mouse chromosome 4 controls a new surface alloantigen. *Immunogenetics* 13: 539–546.
27. Tokushige, K., K. Kinoshita, S. Hirose, and T. Shirai. 1992. Genetic association between natural autoantibody responses to histones and DNA in murine lupus. *Autoimmunity* 12: 285–293.
28. Nomura, T., H. Han, M. C. Howard, H. Yagita, H. Yakura, T. Honjo, and T. Tsubata. 1996. Antigen receptor-mediated B cell death is blocked by signaling via CD72 or treatment with dextran sulfate and is defective in autoimmunity-prone mice. *Int. Immunol.* 8: 867–875.
29. Onodera, T., J. C. Poe, T. F. Tedder, and T. Tsubata. 2008. CD22 regulates time course of both B cell division and antibody response. *J. Immunol.* 180: 907–913.
30. Rolink, A., F. Melchers, and J. Andersson. 1996. The SCID but not the *RAG-2* gene product is required for S μ-S ε heavy chain class switching. *Immunity* 5: 319–330.
31. Heit, A., K. M. Huster, F. Schmitz, M. Schiemann, D. H. Busch, and H. Wagner. 2004. CpG-DNA aided cross-priming by cross-presenting B cells. *J. Immunol.* 172: 1501–1507.
32. Napirei, M., H. Karsunky, B. Zevnik, H. Stephan, H. G. Mannherz, and T. Möröy. 2000. Features of systemic lupus erythematosus in Dnase1-deficient mice. *Nat. Genet.* 25: 177–181.
33. Knight, J. G., D. D. Adams, and H. D. Purves. 1977. The genetic contribution of the NZB mouse to the renal disease of the NZB x NZW hybrid. *Clin. Exp. Immunol.* 28: 352–358.
34. Ogimoto, M., G. Ichinowatari, N. Watanabe, N. Tada, K. Mizuno, and H. Yakura. 2004. Impairment of B cell receptor-mediated Ca^{2+} influx, activation of mitogen-activated protein kinases and growth inhibition in CD72-deficient BAL-17 cells. *Int. Immunol.* 16: 971–982.
35. Li, D. H., M. M. Winslow, T. M. Cao, A. H. Chen, C. R. Davis, E. D. Mellins, P. J. Utz, G. R. Crabtree, and J. R. Parnes. 2008. Modulation of peripheral B cell tolerance by CD72 in a murine model. *Arthritis Rheum.* 58: 3192–3204.
36. Oishi, H., T. Tsubaki, T. Miyazaki, M. Ono, M. Nose, and S. Takahashi. 2013. A bacterial artificial chromosome transgene with polymorphic Cd72 inhibits the development of glomerulonephritis and vasculitis in MRL-Faslpr lupus mice. *J. Immunol.* 190: 2129–2137.
37. Hsu, A. P., K. C. Dowdell, J. Davis, J. E. Niemela, S. M. Anderson, P. A. Shaw, V. K. Rao, and J. M. Puck. 2012. Autoimmune lymphoproliferative syndrome due to FAS mutations outside the signal-transducing death domain: molecular mechanisms and clinical penetrance. *Genet. Med.* 14: 81–89.
38. Hitomi, Y., N. Tsuchiya, A. Kawasaki, J. Ohashi, T. Suzuki, C. Kyogoku, T. Fukazawa, S. Bejrachandra, U. Siriboonrit, D. Chandanayingyong, et al. 2004. *CD72* polymorphisms associated with alternative splicing modify susceptibility to human systemic lupus erythematosus through epistatic interaction with *FCGR2B*. *Hum. Mol. Genet.* 13: 2907–2917.
39. Hitomi, Y., T. Adachi, N. Tsuchiya, Z. I. Honda, K. Tokunaga, and T. Tsubata. 2012. Human CD72 splicing isoform responsible for resistance to systemic lupus erythematosus regulates serum immunoglobulin level and is localized in endoplasmic reticulum. *BMC Immunol.* 13: 72.
40. Izui, S., M. Higaki, D. Morrow, and R. Merino. 1988. The Y chromosome from autoimmune BXSB/MpJ mice induces a lupus-like syndrome in (NZW x C57BL/6)F1 male mice, but not in C57BL/6 male mice. *Eur. J. Immunol.* 18: 911–915.
41. Wakeland, E. K., K. Liu, R. R. Graham, and T. W. Behrens. 2001. Delineating the genetic basis of systemic lupus erythematosus. *Immunity* 15: 397–408.
42. Jiang, Y., S. Hirose, M. Abe, R. Sanokawa-Akakura, M. Ohtsuji, X. Mi, N. Li, Y. Xiu, D. Zhang, J. Shirai, et al. 2000. Polymorphisms in IgG Fc receptor IIB regulatory regions associated with autoimmune susceptibility. *Immunogenetics* 51: 429–435.
43. Pritchard, N. R., A. J. Cutler, S. Uribe, S. J. Chadban, B. J. Morley, and K. G. Smith. 2000. Autoimmune-prone mice share a promoter haplotype associated with reduced expression and function of the Fc receptor FcgammaRII. *Curr. Biol.* 10: 227–230.
44. Tsubata, T. 1999. Co-receptors on B lymphocytes. *Curr. Opin. Immunol.* 11: 249–255.
45. Smith, K. G., and M. R. Clatworthy. 2010. FcgammaRIIB in autoimmunity and infection: evolutionary and therapeutic implications. *Nat. Rev. Immunol.* 10: 328–343.
46. Kumanogoh, A., C. Watanabe, I. Lee, X. Wang, W. Shi, H. Araki, H. Hirata, K. Iwahori, J. Uchida, T. Yasui, et al. 2000. Identification of CD72 as a lymphocyte receptor for the class IV semaphorin CD100: a novel mechanism for regulating B cell signaling. *Immunity* 13: 621–631.

 DOI: 10.1002/eji.201243057 Eur. J. Immunol. 2013. 43: 770–778

European Journal of Immunology

Phenotype conversion from rheumatoid arthritis to systemic lupus erythematosus by introduction of *Yaa* mutation into FcγRIIB-deficient C57BL/6 mice

Shinya Kawano[*1], *Qingshun Lin*[*2], *Hirofumi Amano*[1], *Toshiyuki Kaneko*[1], *Keiko Nishikawa*[2], *Hiromichi Tsurui*[2], *Norihiro Tada*[3], *Hiroyuki Nishimura*[4], *Toshiyuki Takai*[5], *Toshikazu Shirai*[2], *Yoshinari Takasaki*[1] *and Sachiko Hirose*[2]

[1] Department of Internal Medicine, Juntendo University School of Medicine, Tokyo, Japan
[2] Department of Pathology, Juntendo University School of Medicine, Tokyo, Japan
[3] Atopy Research Center, Juntendo University School of Medicine, Tokyo, Japan
[4] Toin Human Science and Technology Center, Department of Biomedical Engineering, Toin University of Yokohama, Yokohama, Japan
[5] Department of Experimental Immunology and CREST of JST, Institute of Development, Aging and Cancer, Tohoku University, Sendai, Japan

We previously established an IgG Fc receptor IIB (FcγRIIB)-deficient C57BL/6 (B6)-congenic mouse strain (KO1), which spontaneously develops rheumatoid arthritis (RA), but not systemic lupus erythematosus (SLE). Here, we show that when Y chromosome-linked autoimmune acceleration (*Yaa*) mutation was introduced in KO1 strain (KO1.*Yaa*), the majority of KO1.*Yaa* mice did not develop RA, but instead did develop SLE. This phenotype conversion did not depend on autoantibody specificity, since KO1.*Yaa* mice, compared with KO1, showed a marked increase in serum levels of both lupus-related and RA-related autoantibodies. The increase in frequencies of CD69$^+$ activated B cells and T cells, and the spontaneous splenic GC formation with T follicular helper cell generation were manifest early in life of KO1.*Yaa*, but not KO1 and B6.*Yaa*, mice. Activated CD4$^+$ T cells from KO1.*Yaa* mice showed upregulated production of IL-21 and IL-10, compared with the finding in KO1 mice, indicating the possibility that this aberrant cytokine milieu relates to the disease phenotype conversion. Thus, our model is useful to clarify the shared and the disease-specific mechanisms underlying the clinically distinct systemic autoimmune diseases RA and SLE.

Keywords: Cytokines · FcγRIIB receptor · Rheumatoid arthritis · Systemic lupus erythematosus · *Yaa* mutation

Introduction

IgG Fc receptor IIB (FcγRIIB) is a major negative regulator of BCR-mediated activation signals in B cells [1]. We previously found that the *Fcgr2b* gene encoding FcγRIIB is polymorphic, and that autoimmune disease-prone mouse strains, such as NZB, BXSB, MRL, and NOD, all share deletion polymorphism in the AP-4-binding site in the *Fcgr2b* promoter region [2]. Because of the

Correspondence: Prof. Sachiko Hirose
e-mail: sacchi@juntendo.ac.jp

*These authors contributed equally to this work.

defective AP-4 binding, mice with this autoimmune-type allele polymorphism show downregulation of FcγRIIB expression levels in activated GC B cells, resulting in upregulation of IgG autoantibody production [3, 4]. These observations suggested that the autoimmune-type *Fcgr2b* confers the basis of susceptibility to autoimmune diseases. Consistent was our earlier finding that systemic lupus erythematosus (SLE) phenotypes in BXSB male mice carrying Y chromosome-linked autoimmune acceleration (*Yaa*) mutation were almost completely inhibited by the substitution of the autoimmune-type *Fcgr2b* for the wild C57BL/6 (B6)-type *Fcgr2b* [5]. However, because BXSB female mice carrying the autoimmune-type *Fcgr2b* but lacking *Yaa* did not develop SLE, it is likely that the autoimmune-type *Fcgr2b* contributes to SLE susceptibility through a strong epistatic interaction with *Yaa* mutation.

To examine further the role of the downregulated expression of FcγRIIB in autoimmune diseases, we recently established an FcγRIIB-deficient B6 mouse strain, KO1, by gene targeting in 129-derived embrionic stem cells and selective backcrossing to a B6 background. Intriguingly, KO1 did not develop SLE, but instead developed severe rheumatoid arthritis (RA), as reported previously [6]. This KO1 strain carried a 129-derived approximately 6.3 Mb interval distal from the null-mutated *Fcgr2b* gene within the *Sle16* locus, which is shown to induce loss of self-tolerance in the B6 background [7]. Boross et al. [8] reported that FcγRIIB-deficient B6 mice generated by gene targeting in B6-derived embryonic stem cells, thus lacking the 129-derived flanking *Sle16* locus, fail to develop any sign of autoimmune diseases. Thus, the development of RA in KO1 mice may be due to the epistatic interaction of FcγRIIB deficiency and *Sle16* locus.

Boross et al. [8] also reported that their FcγRIIB-deficient B6 mice develop lethal lupus nephritis in the presence of *Yaa* mutation, indicating the epistatsis between FcγRIIB-deficiency and *Yaa* in the development of full-blown autoimmune diseases. In addition, Subramanian et al. [9] reported that the strong epistatic interaction between *Yaa* and *Sle1*, which contains the autoimmune-predisposing *Slam/Cd2* haplotype, contributes to severe lupus nephritis. The *Sle16* locus also contains this autoimmune-predisposing *Slam/Cd2* haplotype [10].

In contrast to the accelerated effect of *Yaa* on lupus nephritis, Jansson and Holmdahl [11] reported the suppressive effect of *Yaa* on collagen-induced arthritis. In the present study, we have introduced *Yaa* mutation into FcγRIIB-deficient RA-prone KO1 mice to examine how *Yaa* affects the disease phenotypes in these mice. We found that the majority of KO1.*Yaa* mice did not develop RA, but instead did develop severe SLE early in life, and that this phenotype conversion did not depend on the shift of autoantibody specificity from RA-related to lupus-related one.

Characteristic clinical features differ between RA and SLE; however, both diseases share aberrant activation of immune processes associated with the production of a variety of autoantibodies and subsequent immune complex-mediated tissue inflammation. Our model is useful to investigate the shared and the disease-specific factors contributing to the clinically distinct systemic autoimmune diseases RA and SLE.

Results

Disease phenotype in Yaa-carrying FcγRIIB-deficient KO1 mice

KO1 mice developed arthritis after 4 months of age and the disease incidence and severity were increased with age. At 8 months of age, 67% of KO1 mice showed arthritis with marked swelling and stiffness of forepaws and hindpaws. In contrast, the incidence and severity of arthritis were markedly suppressed in KO1.*Yaa* mice and 88% of KO1.*Yaa* mice were free from arthritis (Fig. 1A). Representative macroscopic findings of forepaws and hindpaws of KO1 and KO1.*Yaa* mice at 8 months of age are shown in Figure 1B. Intriguingly, KO1 strain did not develop proteinuria; however, KO1.*Yaa* began to be positive for proteinuria at 2 months of age and the incidence of positive proteinuria reached 63% (Fig. 1C) with 46% mortality rate at 8 months of age (Fig. 1D).

Figure 1E shows a comparison of representative histopathological and immunofluorescent findings of renal glomeruli among B6, B6.*Yaa*, KO1, and KO1.*Yaa* mice at 4 months of age. In KO1.*Yaa* mice, glomeruli were significantly enlarged even at 4 months of age (Fig. 1F), because of a marked cellular proliferation in glomeruli and a large amount of IgG deposition in mesangial area and along glomerular capillary walls. These glomerular lesions were seldom observed in B6, B6.*Yaa*, and KO1 mice even at 8 months of age.

Serum levels of autoantibodies

To examine the relationship between the disease phenotype conversion from RA to SLE and the specificity of autoantibodies, we compared serum levels of lupus-related autoantibodies against dsDNA, chromatin, and RNP, and RA-related rheumatoid factor (RF), anti-type II collagen (CII), and -cyclic citrullinated peptide (CCP) antibodies at 2 and 6 months of age among B6, B6.*Yaa*, KO1, and KO1.*Yaa* mice (Fig. 2). KO1.*Yaa* mice showed higher serum levels of both lupus-related and RA-related autoantibodies than the other three strains of mice even at 2 months of age. The levels of all these antibodies were increased with age in KO1.*Yaa* mice. Age-associated increase was also observed in KO1 mice; however, the levels were remarkably higher in KO1.*Yaa* mice than those in KO1 mice at 6 months of age. Thus, the conversion of disease phenotype from RA to SLE was not explained by the shift of antibody specificity from RA-type to lupus-type.

Splenomegaly, subpopulation, and maturation/activation status of splenic lymphocytes

The spleen weight in B6, B6.*Yaa*, KO1, and KO1.*Yaa* mice was compared at 4 months of age. Splenomegaly was only observed in KO1.*Yaa* mice (Fig. 3A). Consistently, spontaneous GC formation was observed only in KO1.*Yaa* mice at 4 months of age (Fig. 3B).

Flow cytometric analysis of spleen cells from 4-month-old mice revealed that, while there were no differences in

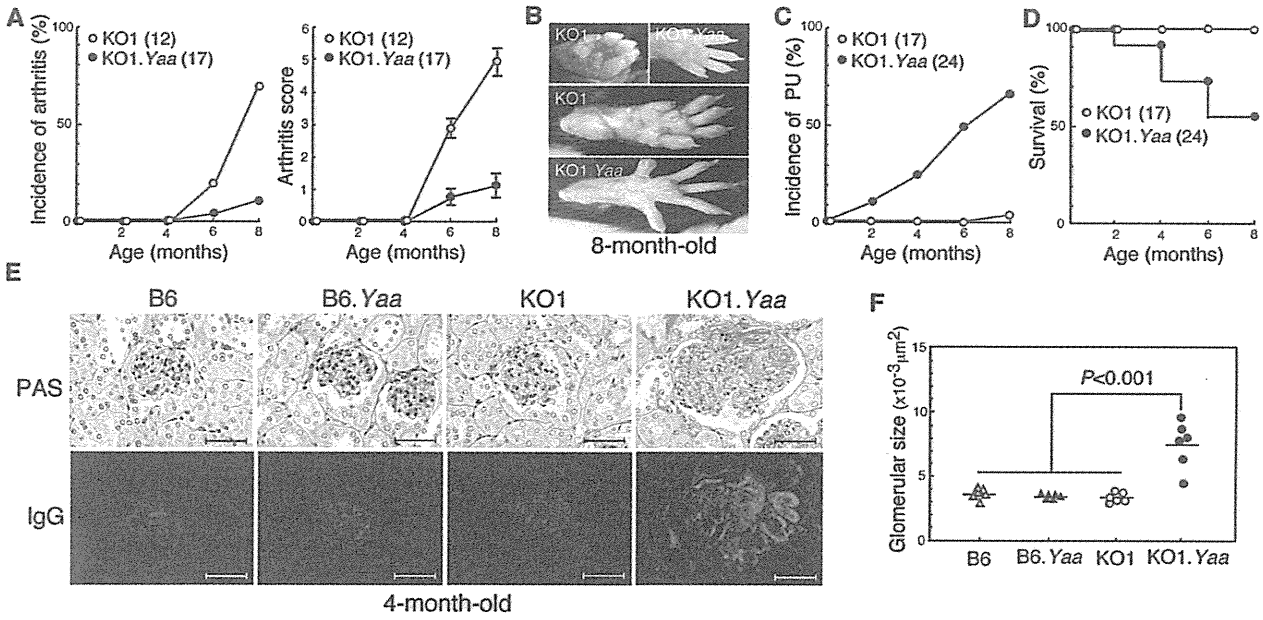

Figure 1. Disease phenotype shift from RA to SLE in KO1.*Yaa* mice. (A) Comparison of the cumulative incidence and score of arthritis between KO1 and KO1.*Yaa* mice. Score is shown as mean ± SE. (B) Representative macroscopic findings of forepaws and hindpaws in KO1 and KO1.*Yaa* mice at 8 months of age. The former mice show marked swelling and stiffness of the wrist and ankle joints. (C) Comparison of the cumulative incidence of proteinuria (PU) between KO1 and KO1.*Yaa* mice. (D) Comparison of survival rate between KO1 and KO1.*Yaa* mice. (E) Histopathological findings of glomeruli in B6, B6.*Yaa*, KO1, and KO1.*Yaa* at 4 months of age. Formalin-fixed sections were stained with periodic acid-Schiff/hematoxylin (PAS) (top). Frozen sections were stained with anti-mouse IgG (bottom) to evaluate the deposition of IgG in renal glomeruli. Scale bars = 50 μm. Representative results obtained from six mice in each strain. (F) Comparison of glomerular size as an indicator of the severity of glomerular lesion. The horizontal bar represents the mean. (A–F) All data are shown as the mean of the indicate numbers of mice in each panel and are representative of three experiments performed. Statistical significance was determined by Mann–Whitney's *U* test.

frequencies of $B220^+$ B cells per total spleen cells among four strains of mice (Table 1), there was a significant decrease in frequencies of $CD21^+CD23^-$ marginal zone B cells in *Yaa*-bearing B6.*Yaa* and KO1.*Yaa* mice (Fig. 4A and Table 1). This decrease is thought to be due to the effect of *Yaa* mutation, as reported previously [12], and not directly related to SLE phenotype. As for the activation/maturation status of B cells, frequencies of $CD69^+$ activated B cells, peanut agglutinin $(PNA)^+$ GC B cells, and $CD138^+$ plasma cells were significantly higher in KO1.*Yaa* mice than those found in other strains of mice (Fig. 4B and Table 1). As for T cells, while total $CD3^+$ T cells per total cells was significantly decreased in KO1.*Yaa* mice, the frequency of $CD69^+$ activated

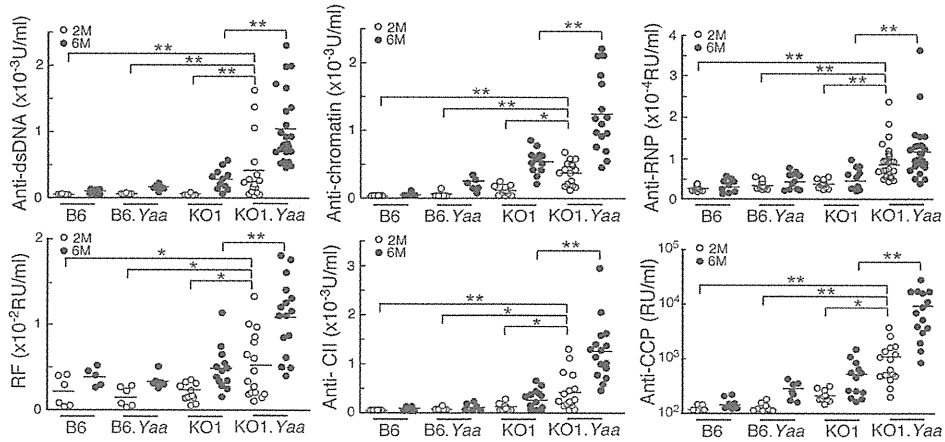

Figure 2. Comparisons of serum levels of lupus-related IgG autoantibodies against dsDNA, chromatin, and RNP, and RA-related IgG RF, anti-CII and -CCP antibodies among B6, B6.*Yaa*, KO1, and KO1.*Yaa* mice at 2 and 6 months of age. Each symbol represents an individual mouse and the bar represents the mean. Data shown are representative of three experiments performed. Statistical significance was determined by Mann–Whitney's *U* test (**$p < 0.001$, *$p < 0.05$).